UNIVERSITÀ DELLA CALABRIA

UNIVERSITA' DELLA CALABRIA

Dipartimento di Ingegneria Informatica, Modellistica, Elettronica e Sistemistica

Scuola di Dottorato

Scienza e Tecnica "Bernardino Telesio"

Indirizzo

Meccanica Computazionale

Con il contributo di POR CALABRIA FSE 2007/2013 Obiettivo Operativo M.2

CICLO

XXVII

BOUNDARY ELEMENT ANALYSIS OF COMPOSITE MATERIALS

Settore Scientifico Disciplinare ICAR/09

Direttore: Ch.mo Prof. Roberto Bartolino

Firma _____

Supervisore: Ch.mo Prof. Raffaele Zinno

Firma _____

Dottorando: Dott. Ferdinando Vetere

Firma _____

Abstract

Nowdays the numerical simulation of mechanical and structural problems in engineering is the method of analysis and design more widespread. Compared to the use of analytical solutions, the numerical simulation is characterized by a great flexibility, due to the possibility to analyze complex geometries and models.

The possibility of finding exact solutions are limited to one-dimensional problems or problems with multiple variables with special symmetries. In the context of the problems of linear elasticity, the situation of isotropic material simplifies the analysis in closed form for the presence of only two elastic coefficients in the constitutive equations. Recently, the interest for the analysis of problems with non-isotropic constitutive equations has been renewed by the availability of new materials suitable for the production of structural elements. In particular, the technical interest in the case of materials with orthotropic constitutive equations.

This work is about the analytical solution of the plane problem for orthotropic materials using a model based on the discretization of the boundary. In order to define the context of the model developed, there is a brief introduction about the method of boundary elements and some considerations on the use of orthotropic materials in structural elements.

Contents

List of Figures

List of Tables

Introduction

The boundary element method

In recent decades, along with the strengthening of the means of calculation, there are well developed methods aimed to construct approximate solutions to complex problems. The common goal of numerical methods is to transform the continuous formulation of the problem in an algebraic form, on the basis of approximate representations of the unknown fields. The discretization methods are classified into domain methods and contour methods, based on the location of the main variables.

Methods belong to the domain methods are the finite difference method, based on direct discretization of the differential quantity, and the finite element method, which today is the most reliable and used means for structural analysis. This method consists in a subdivision of the whole domain into simple elements within which the unknown functions are described through interpolation functions and nodal parameters. Creating a network domain it is often a difficult step in the whole process of solution. It should also be noted that in these methods the variables are distributed over the entire domain, even in the simple case in which it is wanted to know the solution only at one point.

Some of the typical drawbacks of the domain methods are absent in models based on the discretization of the boundary. The basis of these methods is the research work on the boundary integral formulation, which began in the 1800s, when, in the problems of electromagnetism, Green drew the domain information from what was happening on the border of it. His *singularities method* has been applied to problems involving elasticity of the subsequent work of many researchers, including Betti and Somigliana.

After more than a century of research and theoretical developments of analytical solutions, in the 60s of the last century it is started the first numerical applications of this approach with the work of Symm, Rizzo and Shippy [1]. In those same years, the finite element method was developed very quickly, perhaps because of its greater simplicity.

The current name of this method (Boundary Element Method) is due in Brebbia, which since the 70s has contributed to the spread of the method.

The positive characteristics that make this method competitive in comparison to domain methods are:

- The domain is discretized only in cases where data require it.
- The use of the variables is optimized, both because the formulation on the contour reduces size of the problem and because it is possible to concentrate the computational resources only in the area of interest.
- The input stage is very simple, where the finite element method requires a costly and often subjective generation network, which directly influences the accuracy of the solution.

The standard form of the method is based on the location of points on the contour in which resets the residue. Consequently, the method generates algebraic problems governed by non-symmetric matrices.

Anisotropic materials

The elastic isotropy is a possibility of constitutive law that rarely is confirmed by the behavior of real materials. Typically, the behavior of materials depends on their internal structure, whether natural or not artificially induced. Many of the materials found in nature have an anisotropic behavior. These are generally materials that nature produces in time, by overlapping of different layers, which have a determining influence on the blobal mechanical behavior. The ring structure with which the wood grows produces a different behavior along the fibers compared with the behavior detected orthogonally to them. Similarly, the layered structure of the land, with different physical characteristics between each layer, requires the use of an anisotropic models in mechanics of soil and rock. Another type of strong anisotropy is the case of the crystals, which can be categorized according to their directional properties.

In addition to these cases existing in nature, the anisotropy is found in the materials produced artificially, and in particular in materials formed by several components, called composite materials, designed to exploit the characteristics of each component. The different mechanical properties of the components and the manner in which they are combined are the causes of the anisotropy of the composite. The coupling between resistant but brittle materials and ductile but less resistant materials, is a technique revived in time in different forms. An example is the bricks of clay and straw, or iron chains embedded in the walls, to the reinforced concrete to modern fiber-reinforced.

Many composite materials are made up of continuous matrices and discontinuous reinforcements embedded in them. The reinforcements can take many

forms: foils, fibers, flakes, etc. The orientation and geometry of the reinforcement govern the mechanical behavior of the system in different directions.

The laminated materials are a apart category and they are made of overlapping plates that differ in the type or material, or more frequently in the orientation of the fibers. The orientation of the fibers, the material which constitutes them and the material used for adhesive, contribute to determining the characteristics of the product. The laminated wood is an example of how this technique can lead to better quality than the original material.

In the context of the problem treated in this work, it should be noted that the assumption of homogeneity of the body requires to make a homogenization of the mechanical properties. Among the various types of composites are of interest those that are used in the construction of shells in the aerospace industry such as aircraft, missiles and launcher that have an orthotropic behavior.

Objectives and contents of the thesis

The problem of plane orthotropy has been treated in recent years by many researchers with a BEM approach. The work that marked the beginning of this research is the article of Rizzo and Shippy [1] which was also one of the first works where the fundamental solutions for the anisotropic materials were introduced. Recently the fundamental solutions for orthotopic plane problems were improved by Szeidl and Huang [2, 3]. In these works it is used a numerical integration to compute the boundary coefficients.

An analytical evaluation of the boundary coefficients it is used in the 2-D isotropic plane and bending problem by Aristodemo and Turco [4, 5].

The mechanical problem that this thesis deals with is the plane orthotropy. The aim is to furnish an accurate evaluation of the stress field at low computational cost. Numerical efficiency is achieved by refining the boundary interpolation and the integration process. The boundary mechanical quantities are described by means of macro-elements on which a quadratic HC-spline approximation ensures a C1 continuity using few control points. By considering linear piecewise boundaries, the analytical integration of coefficients is carried out. The exact evaluation of integrals is decisive for an accurate computation of the inner stress field from the boundary solution.....

1

Composite Materials

Nowdays the orthotropic materials (e.g. composite materials) are extensively used in modern industries. The theory of elasticity for orthotropic bodies is well established [6, 7, 8], and subsequently more complicated elastic problems of orthotropic bodies have also been studied with numerical methods, such as the Finite Element Method (FEM) [9] and the Boundary Element Method (BEM).

In the following chapter is briefly resumed the theory which is the basis of the composite materials.

1.1 Types and property

Composite materials are materials made from two or more constituent materials with significantly different physical or chemical properties, that when combined, produce a material with characteristics different from the individual components. The individual components remain separate and distinct within the finished structure. The new material may be preferred for many reasons: common examples include materials which are stronger, lighter or less expensive when compared to traditional materials.

Usually a composite is made by immersing a discontinuous phase in a continuous phase. the continuous phases is called *matrice*, the discontinuous one is called *reinforcement*. The matrice is the phase that gives to the composite the shape and its scope is to inglobe the reinforcement material that confers to the composite the main structural behavior. Usually, the reinforcement has these shape: fiber, particle, flakes, laminae.

A lot of materials are made for increasing both the mechanical characteristics and the resistance and the stiffness, as well as the thermal characteristics. The resistance mechanism depends on the geometry and the type of the reinforcement, so, it is common to classify the materials depending on the geometry and the used reinforcement material. So, we have the following composite material

- Composites made by fibers, where the reinforcement is made by one or more types of fiber, with or without matrice
- Composites made by flakes
- Composites made by particle
- Laminates, composed by assembling, with various way, of layers of reduced thickness called lamine.

The characteristic of the composite material depends

- from the nature of the material that composes the reinforcement
- from the shape and the structural distribution of the reinforcement
- from the interaction between the constituents.

The dependence from the nature of the reinforcement is obvious. the structural characteristic, how the reinforcement is distributed in the matrix, and geometrical, in other words the geometrical shape, they play a essential role in the global behavior of the composite. The orientation of the reinforcement governs the isotropy of the system. When the reinforcement has the shape of particle or it is composed by fibers with a reduced length and random orientation, the composite behaves like a isotropic material. Instead, the composites that have an oriented distribution of the fibers show an evidently anisotropic behavior linked to the orientation of the reinforcement. The mechanical properties of the composite in one direction, stiffness and strength, are linked to the amount of fibers oriented in that direction.

In many cases the anisotropy is, linked to the used to a material is intended, a desirable characteristic for the composite. The advantages are linked to the fact that the anisotropy is controlled. So, depending on the constituent characteristics and to the production process, it is possible to regulate the level of the desired anisotropy.

Since the bigger level of anisotropy is represented by the fiber-reinforced composites and by the laminates, it is useful to show detailing these types of composites.

1.2 Fiber-reinforced composites

They are used different kinds of fibers depending on to the requisites required by the composite. Below, it is made a list of the different kind of fibers that are generally used in the building of the structural materials.

- Glass fibers. They are usually coupled with a polymer matrice. The advantages are the low cost and the high strength of the material. However, they have a low abrasion resistance and a poor attitude accession with matrices of polymer resins.

- Carbon and Graphite fibers. The graphite fibers are mainly used for the production of composites with high performances produced by their high mechanical characteristics, both in stiffness and in strength. The word "carbon fibers" and "graphite fibers" is used to indicate the same chemical structure but with different amount of fibers.

- Aramid fibers. These kind of fibers have a high tensile strength but a low compression strength.

- Boron fibers. they are used as a reinforcement in the polymer and metal matrices. There are two types of fibers: with tungsten and with carbon.

The role of the matrice is to link the fibers each other, and to transert to them the tensions and to protect them from the aggressive agents. The role of the matrice, in term of strength and stiffness, depends on the orientation and the sign of the stresses. In the transverse direction to the fibers it produces an important role both for the compression stress and for the tensile stress, while in the fiber direction it essentially induces on the compressive stiffness and strength. They are used the following types of matrice

- Polymeric matrices. The polymers are the more popular materials for the realization of matrices for fiber composites. Their advantages are low costs, simplicity of the process, resistance against chemical attacks, low weight. They are downsides the poor stiffness and strength and the rapid degradation caused by exposure of UVA and some solvents. Some kind of polymers used are the polyester resins and epoxy resins.

- Metal matrices. They are commonly used for their high strength and stiffness, and also for their high impact resistance and for their non-insensitivity to thermal gradients. The use is limited for their weight and for their complicated production process.

1.3 The laminates

A laminate is a collection of laminae stacked to achieve the desired stiffness and thickness. The sequence of various orientations of a fiber-reinforced composite layer in a laminate is termed the lamination scheme or stacking sequence. The layers are usually bonded together with the same matrix material as that in a lamina. The lamination scheme and material properties of individual lamina provide an added flexibility to designers to tailor the stiffness and strength of the laminate to match the structural stiffness and strength requirements. Laminates made of fiber-reinforced composite materials also have disadvantages. Because of the mismatch of material properties between layers, the shear stresses produced between the layers, especially at the edges of a laminate, may cause delamination. Similarly, because of the mismatch of material properties between matrix and fiber, fiber debonding may take place.

Also, during manufacturing of laminates, material defects such as interlaminar voids, delamination, incorrect orientation, damaged fibers, and variation in thickness may be introduced. It is impossible to eliminate manufacturing defects altogether; therefore, analysis and design methodologies must account for various mechanisms of failure.

1.4 Elastic costants based on micromechanics

The aim is to predict the material constants of a composite material by studying the micromechanics of the problem, i.e. by studying how the matrix and fibers interact. Computing the stresses within the matrix, within the fiber, and at the interface of the matrix and fiber is very important for understanding some of the underlying failure mechanisms. In considering the fibers and surrounding matrix, we have the following assumptions

1. Both the matrix and fibers are linearly elastic
2. The fibers are infinitely long
3. The fibers are spaced periodically in square-packed or hexagonal packed arrays.

There are three different approaches that are used to determine the elastic constants for the composite material based on micromechanics. These three approaches are

1. Using numerical models such as the finite element method
2. Using models based on the theory of elasticity
3. Using rule-of-mixtures models based on a strength-of-materials approach.

Consider a unit cell in either a square-packed array (see Fig. 1.1) or a hexagonal-packed array (see Fig. 1.2). The ratio of the cross-sectional area of the fiber to the total cross-sectional area of the unit cell is called the fiber volume fraction and is denoted by V^f . The fiber volume fraction satisfies the relation $0 < V^f < 1$ and is usually 0.5 or greater. Similarly, the matrix volume fraction V^m is the ratio of the cross-sectional area of the matrix to the total cross-sectional area of the unit cell. Note that V^m also satisfies $0 < V^m < 1$. The following relation can be shown to exist between V^f and V^m

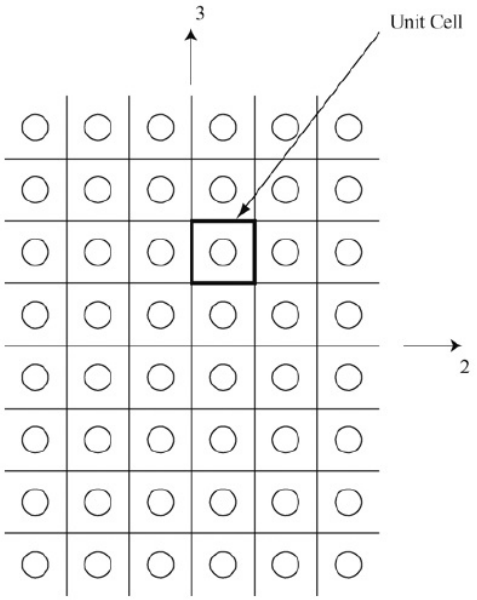

Fig. 1.1. A unit cell in a square-packed array of fiber-reinforced composite material

$$V^f + V^m = 1 \tag{1.1}$$

In the above, we use the notation that a superscript m indicates a matrix quantity while a superscript f indicates a fiber quantity. In addition, the matrix material is assumed to be isotropic so that $E_1^m = E_2^m = E^m$ and $\nu_{12}^m = \nu^m$. However, the fiber material is assumed to be only transversely isotropic such that $E_3^f = E_2^f$, $\nu_{13}^f = \nu_{12}^f$ and $\nu_{23}^f = \nu_{32}^f = \nu^f$.

Using the strength-of-materials approach and the simple rule of mixtures, we have the following relations for the elastic constants of the composite material. For Youngs modulus in the 1-direction (also called the longitudinal stiffness), we have the following relation

$$E_1 = E_1^f V^f + E_1^m V^m \tag{1.2}$$

where E^f is Youngs modulus of the fiber in the 1-direction while E^m is Youngs modulus of the matrix. For Poissons ratio ν_{12}, we have the following relation

$$\nu_{12}^f = \nu_{12}^f V^f + \nu^m V^m \tag{1.3}$$

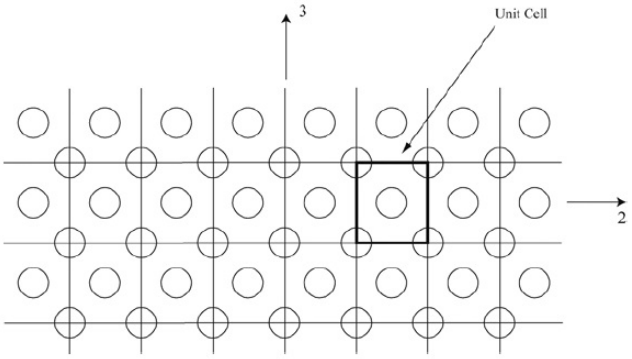

Fig. 1.2. A unit cell in a hexagonal-packed array of fiber-reinforced composite material

where ν_{12}^f and ν^m are Poissons ratios for the fiber and matrix, respectively. For Youngs modulus in the 2-direction (also called the transverse stiffness), we have the following relation

$$\frac{1}{E_2} = \frac{V^f}{E_2^f} + \frac{V^m}{E^m} \tag{1.4}$$

where E_2^f is Youngs modulus of the fiber in the 2-direction while E^m is Youngs modulus of the matrix. For the shear modulus G_{12}, we have the following relation

$$\frac{1}{G_{12}} = \frac{V^f}{G_{12}^f} + \frac{V^m}{G^m} \tag{1.5}$$

where G_{12}^f and G^m are the shear moduli of the fiber and matrix, respectively.

For the coefficients of thermal expansion α_1 and α_2, we have the following relations

$$\alpha_1 = \frac{\alpha_1^f E_1^f V_1^f + \alpha^m E^m V^m}{E_1^f V_1^f + E^m V^m} \tag{1.6}$$

$$\begin{aligned} \alpha_2 = &\left[\alpha_2^f - \left(\frac{E^m}{E_1}\right)\nu_1^f\left(\alpha^m - \alpha_1^f\right)V^m\right]V^f \\ &+ \left[\alpha^m + \left(\frac{E_1^f}{E_1}\right)\nu^m\left(\alpha^m - \alpha_1^f\right)V^f\right]V^m \end{aligned} \tag{1.7}$$

where α_1^f and α_2^f are the coefficients of thermal expansion for the fiber in the 1- and 2-directions, respectively, and α^m is the coefficient of thermal expansion for the matrix. However, we can use a simple rule-of-mixtures relation for α_2^f as follows

$$\alpha_2 = \alpha_2^f V^f + \alpha^m V^m \tag{1.8}$$

A similar simple rule-of-mixtures relation for α_1 cannot be used simply because the matrix and fiber must expand or contract the same amount in the 1-direction when the temperature is changed.

While the simple rule-of-mixtures models used above give accurate results for E^1 and ν_{12}, the results obtained for E_2 and G_{12} do not agree well with finite element analysis and elasticity theory results. Therefore, we need to modify the simple rule-of-mixtures models shown above. For E_2, we have the following modified rule-of-mixtures formula:

$$\frac{1}{E_2} = \frac{\dfrac{V^f}{E_2^f} + \dfrac{\eta V^m}{E^m}}{V^f + \eta V^m} \tag{1.9}$$

where η is the stress-partitioning factor (related to the stress σ_2). This factor satisfies the relation $0\eta < 1$ and is usually taken between 0.4 and 0.6.

Another alternative rule-of-mixtures formula for E^2 is given by

$$\frac{1}{E_2} = \frac{\eta^f V^f}{E_2^f} + \frac{\eta^m V^m}{E^m} \tag{1.10}$$

where the factors η^f and η^m are given by

$$\eta^f = \frac{E_1^f V^f + \left[\left(1 - \nu_{12}^f \nu_{21}^f\right) E^m + \nu^m \nu_{12}^f E_1^f\right] V^m}{E_1^f V^f + E^m V^m} \tag{1.11}$$

$$\eta^m = \frac{\left[\left(1 - \nu^{m^2}\right) E_1^f - \left(1 - \nu^m \nu_{12}^f\right) E^m\right] V^f + E^m V^m}{E_1^f V^f + E^m V^m} \tag{1.12}$$

The above alternative model for E_2 gives accurate results and is used whenever the modified rule-of-mixtures model of 1.9 cannot be applied, i.e. when the factor η is not known.

The modified rule-of-mixtures model for G_{12} is given by the following formula

$$\frac{1}{G_{12}} = \frac{\dfrac{V^f}{G_{12}^f} + \dfrac{\eta' V^m}{G^m}}{V^f + \eta' V^m} \tag{1.13}$$

where η' is the shear stress-partitioning factor. Note that η' satisfies the relation $0 < \eta' < 1$ but using $\eta' = 0.6$ gives results that correlate with the elasticity solution.

Finally, the elasticity solution gives the following formula for G_{12}

$$G_{12} = G^m \frac{\left[\left(G^m + G_{12}^f\right) - V^f\left(G^m - G_{12}^f\right)\right]}{\left[\left(G^m + G_{12}^f\right) + V^f\left(G^m - G_{12}^f\right)\right]} \tag{1.14}$$

2

Plane Elasticity

2.1 Plane stress

If a thin plate is loaded by forces applied at the boundary, parallel to the plane of the plate and distributed uniformly over the thickness (see Fig. 2.1), the stress components σ_{zz}, τ_{xz} and τ_{yz} are zero on both faces of the plate, and it may be assumed, tentatively, that they are zero also within the plate. The state of stress is then specified by σ_{xx}, σ_{yy} and τ_{xy} only, and it is called plane stress. It also be assumed that these three components are independent of z, i.e., they do not vary through the thickness. They are function of x and y only.

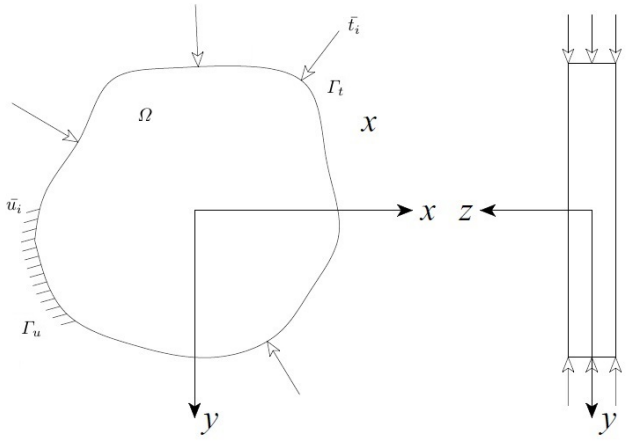

Fig. 2.1. Plane stress

In a reference system (x, y) it is considered a body which occupies a domain Ω surrounded by a border Γ. The body is subject to the actions $\bar{t_i}$ on the portion of the free boundary Γ_t, to the conditions on the displacement $\bar{u_i}$ on the portion of bound contour Γ_u and to the volume actions b_i in the domain Ω. The solution must verify the following equations

- Equilibrium Equation

$$\sigma_{ij,j} + b_i = 0 \qquad in \qquad \Omega \tag{2.1a}$$

$$\sigma_{ij} n_j = \bar{t_i} \qquad on \qquad \Gamma_t \tag{2.1b}$$

- Kinematic Equations

$$\epsilon_{ij} = \frac{1}{2}\left(u_{i,j} + u_{j,i}\right) \qquad in \qquad \Omega \tag{2.2a}$$

$$u_i = \bar{u_i} \qquad on \qquad \Gamma_t \tag{2.2b}$$

- Hooke's Law

$$\sigma_{ij} = C_{ijhk}\epsilon_{hk} \tag{2.3}$$

2.2 Othotropic plane stress

Considering an orthotropic elastic body, which is described by a rectangular Cartesian coordinates $[x_1, x_2]$. The behavior of the body is described by the two-dimensional fields of displacement, stress and strain. So, the equations written above become

- Equilibrium Equation

$$\sigma_{ij,j} + b_i = 0 \tag{2.4}$$

- Kinematic Equations

$$\epsilon_{ij} = \frac{1}{2}\left(u_{i,j} + u_{j,i}\right) \tag{2.5}$$

- Hooke's Law

$$\begin{aligned} \sigma_{11} &= C_{11}\epsilon_{11} + C_{12}\epsilon_{22} \\ \sigma_{22} &= C_{12}\epsilon_{11} + C_{22}\epsilon_{22} \\ \sigma_{12} &= C_{33}\epsilon_{12} + C_{66}\epsilon_{66} \end{aligned} \tag{2.6}$$

where C_{ij} are the components of the stiffness matrix

$$\begin{gathered} C_{11} = S_{22}/d \qquad C_{12} = C_{21} = -S_{12}/d \qquad C_{22} = S_{11}/d \\ C_{66} = 1/S_{66} \qquad d = S_{11}S_{22} - S_{12}^2 \end{gathered} \tag{2.7}$$

and S_{ij} are the components of the compliance matrix.

2.3 Fundamental Solutions

The formulation of the boundary integral equations requires knowledge of the exact solution of the problem on an infinite elastic domain loaded in a punctual way. Rizzo and Shippy [1] have derived the fundamental solution for an anisotropic body from the Navier's equations. Later, this solution was improved and extended to a orthotropic body by Szeild, Huang and all. [2, 3].

So, it's considered an elastic orthotropic plane problem on an infinite domain, under a concentrated force $\mathbf{f}^*$ applied in an its point. The fundamental solutions of this problem it is obtained integrating the equations that are rewritten in the Navier's equilibrium form

$$Lu + b = 0 \tag{2.8}$$

where L is the differential operator in Navier's form

$$\left[L\right] = \begin{bmatrix} C_{11}\partial_1^2 + C_{66}\partial_2^2 & (C_{11} + C_{66})\,\partial_1\partial_2 \\ (C_{11} + C_{66})\,\partial_1\partial_2 & C_{22}\partial_2^2 + C_{66}\partial_1^2 \end{bmatrix} \tag{2.9}$$

solving the system (2.9) it's possible to obtain the fundamental solutions.

$$\begin{aligned} u_{11}(\xi, x) &= D\left[\sqrt{\lambda_1}\, A_2^2 \ln z_1 - \sqrt{\lambda_2}\, A_1^2 \ln z_2\right] \\ u_{12}(\xi, x) &= DA_1A_2\left[\arctan\left(\frac{r_2}{\sqrt{\lambda_2}r_1}\right) - \arctan\left(\frac{r_2}{\sqrt{\lambda_1}r_1}\right)\right] \\ u_{21}(\xi, x) &= u_{12}(\xi, x) \\ u_{22}(\xi, x) &= -D\left[\frac{A_1^2}{\sqrt{\lambda_1}} \ln z_1 - \frac{A_2^2}{\sqrt{\lambda_2}} \ln z_2\right] \end{aligned} \tag{2.10}$$

Using the constitution law stress-strain you have

$$
\begin{aligned}
\sigma_{111} &= D\left[\sqrt{\lambda_2}A_1\frac{r_1}{z_2^2} - \sqrt{\lambda_1}A_2\frac{r_1}{z_1^2}\right] \\
\sigma_{122} &= D\left[\lambda_1\sqrt{\lambda_1}A_2\frac{r_1}{z_1^2} - \lambda_2\sqrt{\lambda_2}A_1\frac{r_1}{z_2^2}\right] \\
\sigma_{121} &= D\left[\sqrt{\lambda_2}A_1\frac{r_2}{z_2^2} - \sqrt{\lambda_1}A_2\frac{r_2}{z_1^2}\right] \\
\sigma_{112} &= \sigma_{121} \\
\sigma_{211} &= D\left[\frac{A_2}{\sqrt{\lambda_2}}\frac{r_2}{z_2^2} - \frac{A_1}{\sqrt{\lambda_1}}\frac{r_2}{z_1^2}\right] \\
\sigma_{222} &= D\left[\sqrt{\lambda_1}A_1\frac{r_2}{z_1^2} - \sqrt{\lambda_2}A_2\frac{r_2}{z_2^2}\right] \\
\sigma_{212} &= D\left[\sqrt{\lambda_1}A_1\frac{r_1}{z_1^2} - \sqrt{\lambda_2}A_2\frac{r_1}{z_2^2}\right] \\
\sigma_{212} &= \sigma_{221}
\end{aligned}
\tag{2.11}
$$

So, from the equation (2.1b) you can obtain the tractions

$$
\begin{aligned}
t_{11}(\xi,x) &= D\left[\frac{\sqrt{\lambda_2}A_1}{z_2^2} - \frac{\sqrt{\lambda_1}A_2}{z_1^2}\right](r_1n_1 + r_2n_2) \\
t_{12}(\xi,x) &= D\left\{\left(\frac{\sqrt{\lambda_1}A_1}{z_1^2} - \frac{\sqrt{\lambda_2}A_2}{z_2^2}\right)r_1n_2 - \left(\frac{\sqrt{\lambda_1}}{\lambda_1}\frac{A_1}{z_1^2} - \frac{\sqrt{\lambda_2}}{\lambda_2}\frac{A_2}{z_2^2}\right)r_2n_1\right\} \\
t_{21}(\xi,x) &= D\left\{\left(\frac{\lambda_1\sqrt{\lambda_1}A_2}{z_1^2} - \frac{\lambda_2\sqrt{\lambda_2}A_1}{z_2^2}\right)r_1n_2 - \left(\frac{\sqrt{\lambda_1}A_2}{z_1^2} - \frac{\sqrt{\lambda_2}A_1}{z_2^2}\right)r_2n_1\right\} \\
t_{22}(\xi,x) &= D\left[\frac{\sqrt{\lambda_1}A_1}{z_1^2} - \frac{\sqrt{\lambda_2}A_2}{z_2^2}\right](r_1n_1 + r_2n_2)
\end{aligned}
\tag{2.12}
$$

n_k represent the components of the unit normal at the field point.
The generic term $u^*_{\alpha i}(\xi,x)$ of the fundamental solution represents the component of the displacement of the field point x in x_i direction due to the application at the source point ξ of a unit force directed along x_α. A similar rule applies to the generic component $t^*_{\alpha i}(\xi,x)$.

The coordinate difference between the field point and the source ξ and the field point x is r_k.

$$
r_k(\xi,x) = x_k - \xi_k \tag{2.13}
$$

and

$$\lambda_1 + \lambda_2 = \frac{2S_{12} + S_{66}}{S_{22}} \tag{2.14}$$

$$\lambda_1 \lambda_2 = \frac{S_{11}}{S_{22}} \tag{2.15}$$

$$A_k = S_{11} - \lambda_k S_{22} \tag{2.16}$$

$$z_k^2 = \lambda_k r_1^2 + r_2^2 \tag{2.17}$$

$$D = \frac{1}{2\pi \left(\lambda_1 - \lambda_2\right) S_{22}} \tag{2.18}$$

The equation (2.14) and (2.15) imply

$$\lambda_{1,2} = \frac{2S_{21} + S_{66}}{2S_{22}} \pm \sqrt{\left(\frac{2S_{21} + S_{66}}{2S_{22}}\right)^2 - \left(\frac{S_{11}}{S_{22}}\right)} \tag{2.19}$$

3

Integral formulation of the elastic boundary problems

The search for approximate solutions using numerical techniques is based on a weak formulation of the problem, in which less continuity to the unknown functions is required respect to the differential formulation. In this chapter, the differential form is brought back to an integral form on the contour, within a plane problem of elasticity. It also derived the expression of the tensions in the interior points. The transfer of all the variables and integral terms on the boundary is only the starting point to build a model to boundary elements [10, 11, 12, 13, 14]. The first numerical implementation of the integral equations in elasticity level is due to Rizzo [15].

3.1 Integral weak forms

The equations of the contour is obtained starting from the differential form of the equilibrium equations, these are weighed by an appropriate test functions and integrated on the domain on which is defined the problem. Through a series of Gauss's transformation, integrals domain are then transferred, without introducing approximations, on the boundary, ultimately providing a form with variables defined only on contour.

The differential form equilibrium equations of the elastic plane state (2.1a) is weighted by a function u^* and integrated in the domain

$$\int_{\Omega} (\sigma_{ij,j} + b_i)\, u^* \mathrm{d}\Omega = 0 \tag{3.1}$$

The equation obtained (3.1) can be transferred to the boundary Γ of the domain Ω through successive Gauss's transformations. In particular, after the first transforming the integral equation becomes

$$\int_{\Gamma} \sigma_{ij} n_j u_i^* \mathrm{d}\Gamma - \int_{\Omega} \sigma_{ij} u_{i,j}^* \mathrm{d}\Omega = -\int_{\Omega} b_i u_i^* \mathrm{d}\Omega \tag{3.2}$$

A further Gauss's transformation transforms the previous equation in the form

$$\int_{\Gamma} \sigma_{ij} n_j u_i^* \mathrm{d}\Gamma - \int_{\Gamma} \sigma_{ij}^* n_j u_i \mathrm{d}\Gamma + \int_{\Omega} \sigma_{ij,j}^* u_i^* \mathrm{d}\Omega = -\int_{\Omega} b_i u_i^* \mathrm{d}\Omega \tag{3.3}$$

3.2 Somigliana's equation

In equation 3.3 still has two integrals of the domain. However, considering that the volume forces are known functions, the integral on the right-hand side in the equation 3.3 does not introduce any new unknowns. The third integral, however, introduces the displacement variable within the domain, so it is still necessary to work on it. The objective of a contour formulation is to eliminate each domain variable, so, it is appropriate to choose as the weight function the function associated with a concentrated load, represented by a Dirac's delta function Δ which acts on a unlimited domain.

$$\int_{\Omega} \sigma_{ij,j}^* u_i \mathrm{d}\Omega = -\int_{\Omega} \Delta\left[\xi, x\right] e_i u_i \mathrm{d}\Omega = -u_i\left[\xi\right] e_i \tag{3.4}$$

where ξ indicates the source point, x is the field point where the effect is measured and $-u_i\left[\xi\right]$ indicates the displacement components in the point of application of the Dirac's delta function. The solution associated with this concentrated load, called the fundamental solution, has been previously introduced in **Section** 2.3

The stress state on the contour could be represented through the components of the traction vector

$$\sigma_{ij} n_j = t_i \tag{3.5a}$$

$$\sigma_{ij} n_j = t_i^* \tag{3.5b}$$

so, the equation 3.3 can be rewritten as

$$-u_i + \int_{\Gamma} t_i u_i^* \mathrm{d}\Gamma - \int_{\Gamma} t_i^* u_i \mathrm{d}\Gamma = -\int_{\Omega} b_i u_i^* \mathrm{d}\Omega \tag{3.6}$$

known as Somigliana's equation.
Expressing the fundamental solution in the following form

$$u_j^* = u_{ij}^* e_i \tag{3.7a}$$

$$t_j^* = t_{ij}^* e_i \tag{3.7b}$$

the Somigliana's equation can be rewritten as

$$u_i[\xi] = \int_\Gamma u^*_{ij}[\xi, x]\, t_j[x]\, \mathrm{d}\Gamma - \int_\Gamma t^*_{ij}[\xi, x]\, u_j[x]\, \mathrm{d}\Gamma = -\int_\Omega u^*_{ij}[\xi, x]\, b_j \mathrm{d}\Omega \quad (3.8)$$

The equation (3.8) provides a contour integral expression for the displacement field within the domain. To get a model with only contour variables,there is the necessity to particularize this expression bringing to the limit the source point ξ on the boundary.

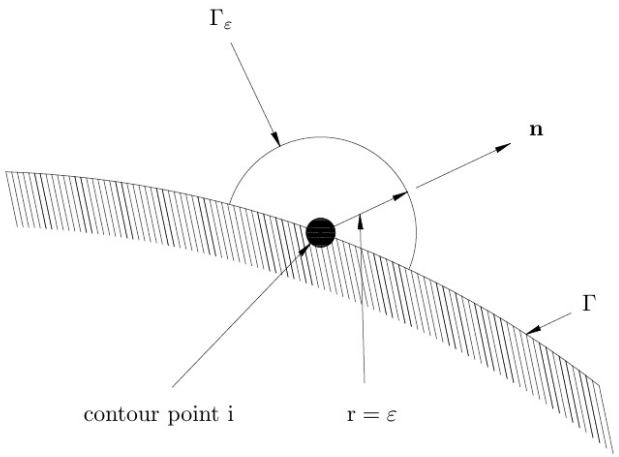

Fig. 3.1. Limit process when the source point is on the boundary

This operation causes the onset of some singularities in the integrals coefficients, that can be evaluate with some simple precautions. You consider the domain extended by a semicircle of radius ε centered on the source as shown in Figure 3.1. Then, the radius ε is brought to zero and it is evaluated separately every single limit of every integrals.

The first integrals doen't have particulary singularity and can be evaluated easily. The second one can be write as

$$\int_\Gamma t^*_{ij}[\xi, x]\, u_j[x]\, \mathrm{d}\Gamma = \lim_{\varepsilon \to 0} \left[\int_{\Gamma - \Gamma_\varepsilon} t^*_{ij}[\xi, x]\, u_j[x]\, \mathrm{d}(\Gamma - \Gamma_\varepsilon) + \int_{\Gamma_\varepsilon} t^*_{ij}[\xi, x]\, u_j[x]\, \mathrm{d}\Gamma \right] \quad (3.9)$$

reaching to the form

$$\lim_{\varepsilon \to 0} \left[\int_{\Gamma - \Gamma_\varepsilon} t^*_{ij} [\xi, x] \, u_j [x] \, \mathrm{d} (\Gamma - \Gamma_\varepsilon) \right] = \int_\Gamma t^*_{ij} [\xi, x] \, u_j [x] \, \mathrm{d}\Gamma \tag{3.10a}$$

$$\int_{\Gamma_\varepsilon} t^*_{ij} [\xi, x] \, u_j [x] \, \mathrm{d}\Gamma = c_{ij} \tag{3.10b}$$

Evaluated the contribution from the singular integral, the rest of the integral, evaluated on the whole boundary except the singular point, then it is to be understood in the sense of the principal value Cauchy. So, the expression of the displacements in a contour point

$$c_{ij} u_i [\xi] = \int_\Gamma u^*_{ij} [\xi, x] \, t_j [x] \, \mathrm{d}\Gamma - \int_\Gamma t^*_{ij} [\xi, x] \, u_j [x] \, \mathrm{d}\Gamma = - \int_\Omega u^*_{ij} [\xi, x] \, b_j \mathrm{d}\Omega \tag{3.11}$$

where the coefficient $c_{ij} [\xi]$ depends on the geometrical characteristics of the boundary in ξ. The coefficient can be specially obtained in closed form. If the tangent is continuous so

$$c_{ij} = \frac{(A_1 - A_2)}{2 (\lambda_1 - \lambda_2) S_{22}} \tag{3.12}$$

The equation 3.11 provides the general equation of the displacement in the domain, it can be also derived to obtain the strain field. Using the constitutive law can eventually be derived stress in interior points

$$\begin{aligned} &\sigma_{ij} [\xi] = \\ &= \int_\Gamma D^*_{ijk} [\xi, x] \, t_k [x] \, \mathrm{d}\Gamma - \int_\Gamma S^*_{ijk} [\xi, x] \, u_k [x] \, \mathrm{d}\Gamma + \int_\Omega D^*_{ijk} [\xi, x] \, b_k [x] \, \mathrm{d}\Omega \end{aligned} \tag{3.13}$$

where the terms concerning the fundamental solution are obtained through the following relations

$$
\begin{aligned}
D_{111} &= D\left[\sqrt{\lambda_2}A_1\frac{r_1}{z_2^2} - \sqrt{\lambda_1}A_2\frac{r_1}{z_1^2}\right] \\
D_{122} &= D\left[\lambda_1\sqrt{\lambda_1}A_2\frac{r_1}{z_1^2} - \lambda_2\sqrt{\lambda_2}A_1\frac{r_1}{z_2^2}\right] \\
D_{121} &= D\left[\sqrt{\lambda_2}A_1\frac{r_2}{z_2^2} - \sqrt{\lambda_1}A_2\frac{r_2}{z_1^2}\right] \\
D_{112} &= D_{121} \\
D_{211} &= D\left[\frac{A_2}{\sqrt{\lambda_2}}\frac{r_2}{z_2^2} - \frac{A_1}{\sqrt{\lambda_1}}\frac{r_2}{z_1^2}\right] \\
D_{222} &= D\left[\sqrt{\lambda_1}A_1\frac{r_2}{z_1^2} - \sqrt{\lambda_2}A_2\frac{r_2}{z_2^2}\right] \\
D_{212} &= D\left[\sqrt{\lambda_1}A_1\frac{r_1}{z_1^2} - \sqrt{\lambda_2}A_2\frac{r_1}{z_2^2}\right] \\
D_{212} &= D_{221}
\end{aligned}
\tag{3.14}
$$

$$
\begin{aligned}
S_{111} &= D\left\{\left[\frac{1}{\sqrt{\lambda_2}z_2^2} - \frac{1}{\sqrt{\lambda_1}z_1^2} - 2\left(\frac{\sqrt{\lambda_2}r_1^2}{z_2^4} - \frac{\sqrt{\lambda_1}r_1^2}{z_1^4}\right)\right]n_1 - 2\left[\frac{\sqrt{\lambda_2}r_1r_2}{z_2^4} - \frac{\sqrt{\lambda_1}r_1r_2}{z_1^4}\right]n_2\right\} \\
S_{112} &= D\left\{-2\left[\frac{\sqrt{\lambda_2}r_1r_2}{z_2^4} - \frac{\sqrt{\lambda_1}r_1r_2}{z_1^4}\right]n_1 + \left[\frac{\sqrt{\lambda_2}}{z_2^2} - \frac{\sqrt{\lambda_1}}{z_1^2} - 2\left(\frac{\sqrt{\lambda_2}r_2^2}{z_2^4} - \frac{\sqrt{\lambda_1}r_2^2}{z_1^4}\right)\right]n_2\right\} \\
S_{121} &= S_{211} = S_{112} \\
S_{122} &= D\left\{\left[\frac{\sqrt{\lambda_1}}{z_1^2} - \frac{\sqrt{\lambda_2}}{z_2^2} + 2\left(\frac{\lambda_2\sqrt{\lambda_2}r_1^2}{z_2^4} - \frac{\lambda_1\sqrt{\lambda_1}r_1^2}{z_1^4}\right)\right]n_1 + 2\left[\frac{\lambda_2\sqrt{\lambda_2}r_1r_2}{z_2^4} - \frac{\lambda_1\sqrt{\lambda_1}r_1r_2}{z_1^4}\right]n_2\right\} \\
S_{212} &= S_{221} = S_{122} \\
S_{222} &= D\left\{2\left[\frac{\lambda_2\sqrt{\lambda_2}r_1r_2}{z_2^4} - \frac{\lambda_1\sqrt{\lambda_1}r_1r_2}{z_1^4}\right]n_1 + \left[\frac{\lambda_1\sqrt{\lambda_1}}{z_1^2} - \frac{\lambda_2\sqrt{\lambda_2}}{z_2^2} + 2\left(\frac{\lambda_2\sqrt{\lambda_2}r_2^2}{z_2^4} - \frac{\lambda_1\sqrt{\lambda_1}r_2^2}{z_1^4}\right)\right]n_2\right\}
\end{aligned}
\tag{3.15}
$$

To generate a discrete model on the basis of the equations (3.11) it is necessary to assume a distribution of the field of displacements and tractions on the contour, taking interpolation functions. By positioning the source at various points along the contour and exploiting more equations of this type, you can obtain a not symmetrical system. On the contuor yo have generally mixed conditions, both on the displacement and on the tractions. So, the

integrals on Γ need to be separated into integrals on Γ_u and into integrals on Γ_t. The vector of unknowns on the contour contains terms of displacement and traction, for which the method has in itself a mixed formulation type. This characteristic has the advantage to lead to accuracies generally comparable, in the calculation of displacements and stresses.

4

Discrete model derived from the integral collocation method

The standard form of the boundary elements method identifies the solution on the boundary of the domain where the problem is defined, through a system of linear algebraic equations, where the associated matrix is not symmetric. The equations of the system, resulting from the formulation, in discrete terms, of the integral equation of the displacements are generated placing on the boundary a number of point sources point equal to the number of interpolation variables. This requires an adequate description boundary geometry, as well as the representation of the mechanical variables of the problem by interpolation functions.

4.1 Discretization of the boundary

As regards the boundary, its geometry can be approximated through the use of curvilinear or linear elements. The first element type ensure a more general modeling, but require, in most cases, the numerical carrying out of the integrals present. The analytical integration is in fact impassable for the complexity of the functions integrands, due to the presence of terms related to the transformations of variables. Linear elements permit an exact description of polygonal contours and, at least in general, they make possible, in a fully analytical way, the development of the integrals involved in the search for a solution on the boundary and in the domain, when the involved kernels are described analytically. It follows a more accurate results and a lower computational time. For these reasons, in what follows reference is made to the discretization of the boundary by straight elements. The process involves the subdivision of the contour in the linear segments (macroelements). These macroelements are also internally divided into several elements (Figure 4.1).

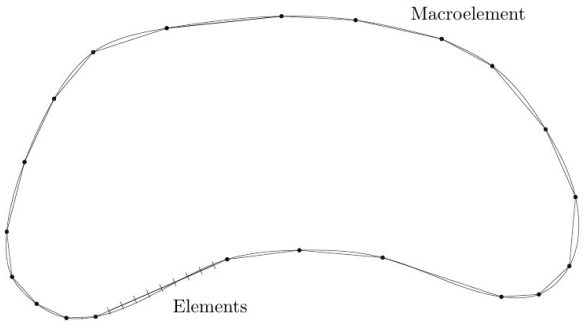

Fig. 4.1. Representation of the contour in straight elements

4.2 Discretization of the mechanical variables

The representation in the discrete form of mechanical variables such as displacement and traction in this case, requires the introduction of the interpolation functions. Within the interpolation functions of polynomial type, it is evident the convenience of obtaining the maximum continuity of the representation using, at the same time, the minimun number of possible parameters.

An interpolation that is proven to help achieve this goal is the so-called interpolation High Continuity (HC) [16], [5]. It is of polynomial functions of B-spline type with C1 continuity. They are constructed by requiring compliance with the continuity conditions both of the variables and their first derivatives at the ends of adjacent elements. This produces the elimination of variables relating to these conditions. Setting to n the number of parameters of piecewise interpolation constant, the HC interpolation needs of a number of parameters equal to $n+2$. So, the i-th components of a vector amount can be described as following

$$f_i\left[\xi\right] = \sum_{k=1}^{3} \phi^{(k)}\left[\xi\right] f_i^{(k)} = \sum_{k=1}^{3} \left(\sum_{h=0}^{2} c_{hk} \left(\xi^{(h)} \right) \right) f_i^{(k)} \tag{4.1}$$

where ξ is an adimensional abscissa on the element, which varies between -1 and 1, $\phi^{(k)}\left[\xi\right]$ is the associated function to the i-th parameter $f_i^{(k)}$, in the node k considered, while, c_{hk} indicates the coefficient of degree h of the polynomial depending by ξ, related to the nodal parameter k.

The general expression of the these functions is

$$\phi_1[\xi] = \frac{1}{4(s+1)}\left(1 - 2\xi + \xi^2\right)$$

$$\phi_2[\xi] = \frac{1}{4(s+1)(d+1)}\left((2 + 3(s+d) + 4sd) + 2(d-s)\xi - (d+s+2)\xi^2\right)$$

$$\phi_3[\xi] = \frac{1}{4(d+1)}\left(1 + 2\xi + \xi^2\right) \tag{4.2}$$

Note the geometric relationships s and d, you can get the three shape functions. When the element of the left or the right one are terminal elements, you insert null values in the expressions for s or d. In this work it will be used only one type of element obtained by setting $s = 1$ and $d = 1$. So, the shape functions for this case are

$$\phi_1[\xi] = \frac{1}{8} - \frac{1}{8}\xi + \frac{1}{8}\xi^2$$

$$\phi_2[\xi] = \frac{3}{4} - \frac{1}{4}\xi^2 \tag{4.3}$$

$$\phi_3[\xi] = \frac{1}{8} + \frac{1}{8}\xi + \frac{1}{8}\xi^2$$

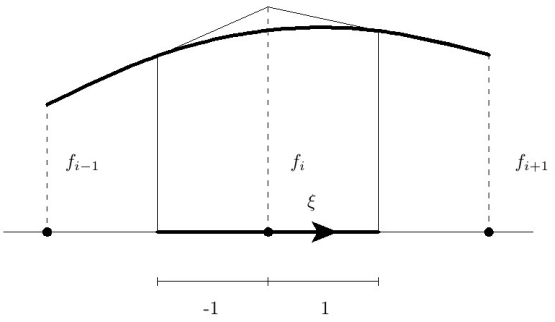

Fig. 4.2. HC element for case s=1 and d=1

4.3 Boundary solution

The discrete form of the equation (3.11) leads to the generation of the system in the contour variables. In particular, using HC interpolation, the displace-

ment and traction fields are represented inside each element by the following relations

$$\begin{aligned} u\left[x\right] &= \phi_{ue} u_e \qquad & u_e^T &= \begin{bmatrix} u_1^{(i-1)} & u_1^{(i)} & u_1^{(i+1)} \\ u_2^{(i-1)} & u_2^{(i)} & u_2^{(i+1)} \end{bmatrix} \\ t\left[x\right] &= \phi_{te} u_e \qquad & t_e^T &= \begin{bmatrix} t_1^{(i-1)} & t_1^{(i)} & t_1^{(i+1)} \\ t_2^{(i-1)} & t_2^{(i)} & t_2^{(i+1)} \end{bmatrix} \end{aligned} \tag{4.4}$$

Finally, taking into account the equation (3.11), it's possible to write the discrete form of the integral equation of the displacement

$$\begin{aligned} c_{ij} u\left(\bar{\xi}\right) + \sum_{e=1}^{n_e} \int_{\Gamma_e} {t^*}^T \left(\xi, x\right) \phi_e u_e \, d\Gamma e = \\ = \sum_{e=1}^{n_e} \int_{\Gamma_e} {u^*}^T \left(\xi, x\right) \phi_e t_e \, d\Gamma e + \sum_{c=1}^{n_c} \int_{\Omega_c} {u^*}^T \left(\xi, x\right) b\left(x\right) d\Omega_c \end{aligned} \tag{4.5}$$

where $\bar{\xi}$ denotes the position of the source, n_e the number of elements in which the contour is divided and n_c is the number of cells in which the domain is divided.

4.4 Research of the solution in the domain

After obtaining the solution on the boundary, it's possible to compute the solution in the interior points of the domain. In particular, to define the displacements field is given from the equation (3.11), but now, the coefficient $c_{ij} = 1$

$$u_i\left[\xi\right] = \int_\Gamma u_{ij}^*\left[\xi, x\right] t_j\left[x\right] \mathrm{d}\Gamma - \int_\Gamma t_{ij}^*\left[\xi, x\right] u_j\left[x\right] \mathrm{d}\Gamma = -\int_\Omega u_{ij}^*\left[\xi, x\right] b_j \mathrm{d}\Omega \tag{4.6}$$

which its discrete form is

$$\begin{aligned} u\left(\xi\right) = \sum_{e=1}^{n_e} \int_{\Gamma_e} {u^*}^T \left(\xi, x\right) \phi_e t_e \, d\Gamma e - \\ - \sum_{e=1}^{n_e} \int_{\Gamma_e} {t^*}^T \left(\xi, x\right) \phi_e u_e \, d\Gamma e + \sum_{c=1}^{n_c} \int_{\Omega_c} {u^*}^T \left(\xi, x\right) b\left(x\right) d\Omega_c \end{aligned} \tag{4.7}$$

The stresses fields is given using the equation 3.13.Its discrete form is

$$\sigma(\xi) = \sum_{e=1}^{n_e} \int_{\Gamma_e} D\phi_e t_e \, d\Gamma e - \sum_{e=1}^{n_e} \int_{\Gamma_e} S\phi_e u_e \, d\Gamma e + \sum_{c=1}^{n_c} \int_{\Omega_c} Db_c(x) \, d\Omega_c \quad (4.8)$$

where

$$D^T = \begin{bmatrix} D_{111} & D_{121} & D_{211} & D_{221} \\ D_{112} & D_{122} & D_{212} & D_{222} \end{bmatrix} \qquad S^T = \begin{bmatrix} S_{111} & S_{121} & S_{211} & S_{221} \\ S_{112} & S_{122} & S_{212} & S_{222} \end{bmatrix} \quad (4.9)$$

which the terms D and S are provided by equation 3.14 and equation 3.15

4.5 Analytical integration of the boundary coefficients

Integral coefficients contained in the equation (4.5) involve the products between the shape functions and the fundamental solutions (2.10) and (2.12). The typical term of integral equations is in the form

$$\int_\Gamma f^* \phi^{(k)}[x] \, \mathrm{d}\Gamma = \sum_{h=0}^{2} c_{hk} \int_{-a}^{a} f_i^* \xi^{(h)} dx \quad (4.10)$$

where the abscissa x is taken in local system centered on the field element, and a indicates the half-length of the field element (see Figure 4.3).

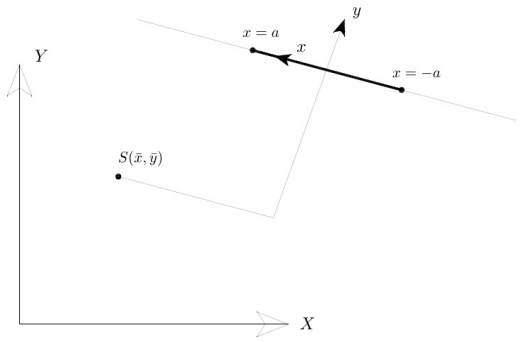

Fig. 4.3. Coordinates of the source point $S(\bar{x}, \bar{y})$ in the local system placed on the element effect

We will make reference to $\bar{x}, \bar{y}$ which are the coordinates of the source point in the local system placed on the field element.

So, the integrals to be computed have the following typical forms

$$\begin{aligned} E(k)_j^{(h)} &= \int_{x_1}^{x_2} \frac{x^h}{(z_k^2)^j} dx \\ G(k)_j^{(h)} &= \int_{x_1}^{x_2} \ln z_k x^h dx \\ A(k)_j^{(h)} &= \int_{x_1}^{x_2} \arctan\left(\frac{\bar{y}}{\sqrt{\lambda_k}\,(x-\bar{x})}\right) dx \end{aligned} \tag{4.11}$$

For the integrals shown in equation (4.11) it is possible to obtain a closed form of the solution. In the calculation of the solution of these integrals you can discern two cases.

4.5.1 Case 1: $n_1 = 0$

The analytical solutions of the indefinite integrals $E(k)_j^{(h)}$ for this case can be posed in the form

$$E(k)_j^{(h)} = \frac{1}{2j-h-1}\left\{\left[\frac{x^{h-1}}{(z_k^2)^{j-1}}\right]_{x_1}^{x_2} + 2\bar{x}\,(j-h)\,E(k)_j^{(h-1)} + (h-1)\left(\lambda_k\bar{x}^2+\bar{y}^2\right)E(k)_j^{(h-2)}\right\} \tag{4.12}$$

in particular, when $k = 2j-1$, it is necessary to use the following equation

$$E(k)_j^{(h)} = E(k)_{j-1}^{(h-2)} - \left(\lambda_k\bar{x}^2+\bar{y}^2\right)E(k)_j^{(h-2)} + 2\bar{x}E(k)_j^{(h-1)} \tag{4.13}$$

The integrals needed to initialize the recursive process when $\bar{y} \neq 0$ are

$$E(k)_1^{(0)} = \frac{1}{\sqrt{\lambda_k}\bar{y}}\left[arctan\left(\frac{\sqrt{\lambda_k}\,(x-\bar{x})}{\bar{y}}\right)\right]_{x_1}^{x_2} \tag{4.14a}$$

$$E(k)_1^{(1)} = \frac{1}{\sqrt{\lambda_k}}\left[ln\,(z_k)\right]_{x_1}^{x_2} + \bar{x}E(k)_1^{(0)} \tag{4.14b}$$

$$E(k)_0^{(h)} = \left[\frac{x^{h+1}}{h+1}\right]_{x_1}^{x_2} \tag{4.14c}$$

$$E(k)_{j+1}^{(0)} = \frac{1}{2\bar{y}^2 j}\left\{\left[\frac{(x-\bar{x})}{(z_k^2)^j}\right]_{x_1}^{x_2} + (2j-1)\,E(k)_j^{(0)}\right\} \tag{4.14d}$$

For $\bar{y}=0$ some of these expressions degenerate, and must be replaced with the following

$$E(k)_j^{(0)} = \left[\frac{1}{(x-\bar{x})^{2j-1}}\right]_{x_1}^{x_2}\frac{1}{\lambda_k\,(1-2j)} \tag{4.15}$$

Integrals of type $G(k)_j^{(h)}$ can be represented in closed form. In problem treated is required only the evaluation of integrals $G(k)_0^{(h)}$, which for $\bar{y}\neq 0$ become

$$G(k)_0^{(h)} = \frac{1}{h+1}\left\{\left[ln\,(z_k)\,x^{h+1}\right]_{x_1}^{x_2} - \lambda_k\left(E(k)_1^{(h+2)} - \bar{x}E(k)_1^{(h+1)}\right)\right\} \tag{4.16}$$

when $\bar{y}=0$ it becomes

$$G(k)_0^{(h)} = \frac{1}{h+1}\left\{\left[x^h\left((x-\bar{x})\,ln\,(z_k) - \frac{x}{h+1}\right)\right]_{x_1}^{x_2} + h\bar{x}G(k)_j^{(h-1)}\right\} \tag{4.17}$$

where the first integral of the recursive process is

$$G(k)_0^{(0)} = \left[(x-\bar{x})\,ln\,(z_k) - x\right]_{x_1}^{x_2} \tag{4.18}$$

Even the integrals of type $A(k)_j^{(h)}$ can be represented in closed form. In problem treated is required only the evaluation of integrals $A(k)_0^{(h)}$

$$A(k)_0^{(h)} = \\ = \left[-\frac{h}{h+1}\left(\frac{\bar{x}\bar{y}^{(h-1)}}{\sqrt{\lambda_k}}\right) + \frac{\bar{y}}{2\sqrt{\lambda_k}} ln\left(z_k\right) x^{(h)} + \frac{(h-1)}{6}\frac{\bar{y}^3}{\sqrt{\lambda_k^3}} ln\left(z_k\right) + \right. \\ \left. + \frac{h}{2}\frac{\bar{y}^2}{\lambda_k}\arctan\left(\frac{\sqrt{\lambda_k}\left(x-\bar{x}\right)}{\bar{y}}\right)\bar{x}^{(h-1)} - \arctan\left(\frac{\bar{y}}{\lambda_k\left(x-\bar{x}\right)}\right)\left(\frac{x^{(h+1)}-\bar{x}^{(h+1)}}{h+1}\right)\right]_{x_1}^{x_2} \tag{4.19}$$

where the first integral of the recursive process is

$$A(k)_0^{(0)} = \left[\frac{\bar{y}}{2\sqrt{\lambda_k}} ln\left(z_k\right) - \arctan\left(\frac{\bar{y}}{\lambda_k\left(x-\bar{x}\right)}\right)\left(x-\bar{x}\right)\right]_{x_1}^{x_2} \tag{4.20}$$

The expressions necessary to assemble the system of the boundary equations, depending of the integrals just exposed, are the following

$$U_{11}^{(h)} = D\left[\sqrt{\lambda_1}\, A_2^2 G(1)_0^{(h)} - \sqrt{\lambda_2}\, A_1^2\, G(2)_0^{(h)}\right] \tag{4.21a}$$

$$U_{12}^{(h)} = D A_1 A_2\left[A(2)_0^{(h)} - A(1)_0^{(h)}\right] \tag{4.21b}$$

$$U_{21}^{(h)} = U_{12}^{(h)} \tag{4.21c}$$

$$U_{22}^{(h)} = -D\left[\frac{A_1^2}{\sqrt{\lambda_1}} G(1)_0^{(h)} - \frac{A_2^2}{\sqrt{\lambda_2}} G(2)_0^{(h)}\right] \tag{4.21d}$$

$$T_{11}^{(h)} = \bar{y} D\left[\sqrt{\lambda_2} A_1 E(2)_1^{(h)} - \sqrt{\lambda_1} A_2 E(1)_1^{(h)}\right] \tag{4.21e}$$

$$T_{12}^{(h)} = D\left[\sqrt{\lambda_1} A_1 \tilde{E}(1)_1^{(h)} - \sqrt{\lambda_2} A_2 \tilde{E}(2)_1^{(h)}\right] \tag{4.21f}$$

$$T_{21}^{(h)} = D\left[\lambda_1\sqrt{\lambda_1} A_2 \tilde{E}(1)_1^{(h)} - \lambda_2\sqrt{\lambda_2} A_1 \tilde{E}(2)_1^{(h)}\right] \tag{4.21g}$$

$$T_{22}^{(h)} = \bar{y} D\left[\sqrt{\lambda_1} A_1 E(1)_1^{(h)} - \sqrt{\lambda_2} A_2 E(2)_1^{(h)}\right] \tag{4.21h}$$

where there were inducted

$$\tilde{E}(k)_j^{(h)} = E(k)_j^{(h+1)} - \bar{x} E(k)_j^{(h)} \tag{4.22}$$

As regards the evaluation of the tensions in the interior points, the integral terms of the type D^h_{ijl}, written as a function of the recurring integrals, have the following expressions

$$D^{(h)}_{111} = D\left[\sqrt{\lambda_2}A_1\tilde{E}(2)^{(h)}_1 - \sqrt{\lambda_1}A_2\tilde{E}(1)^{(h)}_1\right] \tag{4.23a}$$

$$D^{(h)}_{122} = D\left[\lambda_1\sqrt{\lambda_1}A_2\tilde{E}(1)^{(h)}_1 - \lambda_2\sqrt{\lambda_2}A_1\tilde{E}(2)^{(h)}_1\right] \tag{4.23b}$$

$$D^{(h)}_{121} = \bar{y}D\left[\sqrt{\lambda_2}A_1E(2)^{(h)}_1 - \sqrt{\lambda_1}A_2E(1)^{(h)}_1\right] \tag{4.23c}$$

$$D^{(h)}_{112} = D^{(h)}_{121} \tag{4.23d}$$

$$D^{(h)}_{211} = \bar{y}D\left[\frac{A_2}{\sqrt{\lambda_2}}E(2)^{(h)}_1 - \frac{A_1}{\sqrt{\lambda_1}}E(1)^{(h)}_1\right] \tag{4.23e}$$

$$D^{(h)}_{222} = \bar{y}D\left[\sqrt{\lambda_1}A_1E(1)^{(h)}_1 - \sqrt{\lambda_2}A_2E(2)^{(h)}_1\right] \tag{4.23f}$$

$$D^{(h)}_{212} = D\left[\sqrt{\lambda_1}A_1\tilde{E}(1)^{(h)}_1 - \sqrt{\lambda_2}A_2\tilde{E}(2)^{(h)}_1\right] \tag{4.23g}$$

$$D^{(h)}_{212} = D^{(h)}_{221} \tag{4.23h}$$

while the integral of the type S^h_{ijl} can be written as

$$S_{111}^{(h)} = -2\bar{y}D\left[\sqrt{\lambda_2}\tilde{E}(2)_2^{(h)} - \sqrt{\lambda_1}\tilde{E}(1)_2^{(h)}\right] \tag{4.24a}$$

$$S_{112}^{(h)} = D\left[\sqrt{\lambda_2}E(2)_1^{(h)} - \sqrt{\lambda_1}E(1)_1^{(h)} - 2\bar{y}^2\left(\lambda_2 E(2)_2^{(h)} - \lambda_1 E(2)_1^{(h)}\right)\right] \tag{4.24b}$$

$$S_{121}^{(h)} = S_{211}^{(h)} = S_{112}^{(h)} \tag{4.24c}$$

$$S_{122}^{(h)} = 2\bar{y}D\left[\lambda_2\sqrt{\lambda_2}\tilde{E}(2)_2^{(h)} - \lambda_1\sqrt{\lambda_1}\tilde{E}(1)_2^{(h)}\right] \tag{4.24d}$$

$$S_{212}^{(h)} = S_{221}^{(h)} = S_{122}^{(h)} \tag{4.24e}$$

$$S_{222}^{(h)} = D\left[\lambda_1\sqrt{\lambda_1}\tilde{E}(1)_1^{(h)} - \lambda_2\sqrt{\lambda_2}\tilde{E}(2)_1^{(h)} + 2\bar{y}^2\left(\lambda_2\sqrt{\lambda_2}E(2)_2^{(h)} - \lambda_1\sqrt{\lambda_1}E(2)_1^{(h)}\right)\right] \tag{4.24f}$$

4.5.2 Case 2: $n_2 = 0$

The analytical solutions of the indefinite integrals $E(k)_j^{(h)}$ for this case can be posed in the form

$$E(k)_j^{(h)} = \frac{1}{2j-h-1}\left\{\left[\frac{x^{h-1}}{(z_k^2)^{j-1}}\right]_{x_1}^{x_2} + 2\bar{x}\,(j-h)\,E(k)_j^{(h-1)} + (h-1)\left(\bar{x}^2 + \lambda_k\bar{y}^2\right)E(k)_j^{(h-2)}\right\} \tag{4.25}$$

in particular, when $k = 2j-1$, it is necessary to use the following equation

$$E(k)_j^{(h)} = E(k)_{j-1}^{(h-2)} - \left(\bar{x}^2 + \lambda_k\bar{y}^2\right)E(k)_j^{(h-2)} + 2\bar{x}E(k)_j^{(h-1)} \tag{4.26}$$

The integrals needed to initialize the recursive process when $\bar{y} \neq 0$ are

$$E(k)_1^{(0)} = \frac{1}{\sqrt{\lambda_k}\bar{y}}\left[arctan\left(\frac{(x-\bar{x})}{\sqrt{\lambda_k}\bar{y}}\right)\right]_{x_1}^{x_2} \tag{4.27a}$$

$$E(k)_1^{(1)} = \left[ln\,(z_k)\right]_{x_1}^{x_2} + \bar{x}E(k)_1^{(0)} \tag{4.27b}$$

$$E(k)_0^{(h)} = \left[\frac{x^{h+1}}{h+1}\right]_{x_1}^{x_2} \tag{4.27c}$$

$$E(k)_{j+1}^{(0)} = \frac{1}{2\lambda_k\bar{y}^2 j}\left\{\left[\frac{(x-\bar{x})}{(z_k^2)^j}\right]_{x_1}^{x_2} + (2j-1)\,E(k)_j^{(0)}\right\} \tag{4.27d}$$

For $\bar{y}=0$ some of these expressions degenerate, and must be replaced with the following

$$E(k)_j^{(0)} = \left[\frac{1}{(x-\bar{x})^{2j-1}}\right]_{x_1}^{x_2}\frac{1}{(1-2j)} \tag{4.28}$$

Integrals of type $G(k)_j^{(h)}$ can be represented in closed form. In problem treated is required only the evaluation of integrals $G(k)_0^{(h)}$, which for $\bar{y}\neq 0$ become

$$G(k)_0^{(h)} = \frac{1}{h+1}\left\{\left[ln\,(z_k)\,x^{h+1}\right]_{x_1}^{x_2} - \left(E(k)_1^{(h+2)} - \bar{x}E(k)_1^{(h+1)}\right)\right\} \tag{4.29}$$

when $\bar{y}=0$ it becomes

$$G(k)_0^{(h)} = \frac{1}{h+1}\left\{\left[x^h\left((x-\bar{x})\,ln\,(z_k) - \frac{x}{h+1}\right)\right]_{x_1}^{x_2} + h\bar{x}G(k)_j^{(h-1)}\right\} \tag{4.30}$$

where the first integral of the recursive process is

$$G(k)_0^{(0)} = \left[(x-\bar{x})\,ln\,(z_k) - x\right]_{x_1}^{x_2} \tag{4.31}$$

Even the integrals of type $A(k)_j^{(h)}$ can be represented in closed form. In problem treated is required only the evaluation of integrals $A(k)_0^{(h)}$

$$A(k)_0^{(h)} = \\ = \left[-\frac{h}{h+1}\left(\frac{\bar{x}\bar{y}^{(h-1)}}{\sqrt{\lambda_k}}\right) + \frac{\bar{y}}{2\sqrt{\lambda_k}} ln\left(z_k\right) x^{(h)} + \frac{(h-1)}{6}\frac{\bar{y}^3}{\sqrt{\lambda_k^3}} ln\left(z_k\right) + \right. \\ \left. + \frac{h}{2}\frac{\bar{y}^2}{\lambda_k}\arctan\left(\frac{\sqrt{\lambda_k}\left(x-\bar{x}\right)}{\bar{y}}\right)\bar{x}^{(h-1)} - \arctan\left(\frac{\bar{y}}{\lambda_k\left(x-\bar{x}\right)}\right)\left(\frac{x^{(h+1)}-\bar{x}^{(h+1)}}{h+1}\right)\right]_{x_1}^{x_2} \tag{4.32}$$

where the first integral of the recursive process is

$$A(k)_0^{(0)} = \left[\frac{\bar{y}}{2\sqrt{\lambda_k}} ln\left(z_k\right) - \arctan\left(\frac{\bar{y}}{\lambda_k\left(x-\bar{x}\right)}\right)\left(x-\bar{x}\right)\right]_{x_1}^{x_2} \tag{4.33}$$

The expressions necessary to assemble the system of the boundary equations, depending of the integrals just exposed, are the following

$$U_{11}^{(h)} = D\left[\sqrt{\lambda_1}\, A_2^2 G(1)_0^{(h)} - \sqrt{\lambda_2}\, A_1^2\, G(2)_0^{(h)}\right] \tag{4.34a}$$

$$U_{12}^{(h)} = DA_1A_2\left[A(2)_0^{(h)} - A(1)_0^{(h)}\right] \tag{4.34b}$$

$$U_{21}^{(h)} = U_{12}^{(h)} \tag{4.34c}$$

$$U_{22}^{(h)} = -D\left[\frac{A_1^2}{\sqrt{\lambda_1}} G(1)_0^{(h)} - \frac{A_2^2}{\sqrt{\lambda_2}} G(2)_0^{(h)}\right] \tag{4.34d}$$

$$T_{11}^{(h)} = \bar{y}D\left[\sqrt{\lambda_2} A_1 E(2)_1^{(h)} - \sqrt{\lambda_1} A_2 E(1)_1^{(h)}\right] \tag{4.34e}$$

$$T_{12}^{(h)} = D\left[\frac{A_1}{\sqrt{\lambda_1}}\tilde{E}(1)_1^{(h)} - \frac{A_2}{\sqrt{\lambda_2}}\tilde{E}(2)_1^{(h)}\right] \tag{4.34f}$$

$$T_{21}^{(h)} = D\left[\sqrt{\lambda_1} A_2 \tilde{E}(1)_1^{(h)} - \sqrt{\lambda_2} A_1 \tilde{E}(2)_1^{(h)}\right] \tag{4.34g}$$

$$T_{22}^{(h)} = \bar{y}D\left[\sqrt{\lambda_1} A_1 E(1)_1^{(h)} - \sqrt{\lambda_2} A_2 E(2)_1^{(h)}\right] \tag{4.34h}$$

where there were inducted

$$\tilde{E}(k)_j^{(h)} = E(k)_j^{(h+1)} - \bar{x}E(k)_j^{(h)} \tag{4.35}$$

As regards the evaluation of the tensions in the interior points, the integral terms of the type D^h_{ijl}, written as a function of the recurring integrals, have the following expressions

$$D^{(h)}_{111} = \bar{y}D\left[\sqrt{\lambda_2}A_1E(2)^{(h)}_1 - \sqrt{\lambda_1}A_2E(1)^{(h)}_1\right] \tag{4.36a}$$

$$D^{(h)}_{122} = \bar{y}D\left[\lambda_1\sqrt{\lambda_1}A_2E(1)^{(h)}_1 - \lambda_2\sqrt{\lambda_2}A_1E(2)^{(h)}_1\right] \tag{4.36b}$$

$$D^{(h)}_{121} = D\left[\sqrt{\lambda_2}A_1\tilde{E}(2)^{(h)}_1 - \sqrt{\lambda_1}A_2\tilde{E}(1)^{(h)}_1\right] \tag{4.36c}$$

$$D^{(h)}_{112} = D^{(h)}_{121} \tag{4.36d}$$

$$D^{(h)}_{211} = D\left[\frac{A_2}{\sqrt{\lambda_2}}\tilde{E}(2)^{(h)}_1 - \frac{A_1}{\sqrt{\lambda_1}}\tilde{E}(1)^{(h)}_1\right] \tag{4.36e}$$

$$D^{(h)}_{222} = D\left[\sqrt{\lambda_1}A_1\tilde{E}(1)^{(h)}_1 - \sqrt{\lambda_2}A_2\tilde{E}(2)^{(h)}_1\right] \tag{4.36f}$$

$$D^{(h)}_{212} = \bar{y}D\left[\sqrt{\lambda_1}A_1E(1)^{(h)}_1 - \sqrt{\lambda_2}A_2E(2)^{(h)}_1\right] \tag{4.36g}$$

$$D^{(h)}_{212} = D^{(h)}_{221} \tag{4.36h}$$

while the integral of the type S^h_{ijl} can be written as

$$S_{111}^{(h)} = D\left[\frac{1}{\sqrt{\lambda_2}}E(2)_1^{(h)} - \frac{1}{\sqrt{\lambda_1}}E(1)_1^{(h)} - 2\bar{y}^2\left(\sqrt{\lambda_2}E(2)_2^{(h)} - \sqrt{\lambda_1}E(1)_2^{(h)}\right)\right] \tag{4.37a}$$

$$S_{112}^{(h)} = -2\bar{y}D\left[\sqrt{\lambda_2}\tilde{E}(2)_2^{(h)} - \sqrt{\lambda_1}\tilde{E}(1)_2^{(h)}\right] \tag{4.37b}$$

$$S_{121}^{(h)} = S_{211}^{(h)} = S_{112}^{(h)} \tag{4.37c}$$

$$S_{122}^{(h)} = D\left[\sqrt{\lambda_1}E(1)_1^{(h)} - \sqrt{\lambda_2}E(2)_1^{(h)} + 2\bar{y}^2\left(\lambda_2\sqrt{\lambda_2}E(2)_2^{(h)} - \lambda_1\sqrt{\lambda_1}E(1)_2^{(h)}\right)\right] \tag{4.37d}$$

$$S_{212}^{(h)} = S_{221}^{(h)} = S_{122}^{(h)} \tag{4.37e}$$

$$S_{222}^{(h)} = 2\bar{y}D\left[\lambda_2\sqrt{\lambda_2}\tilde{E}(2)_2^{(h)} - \lambda_1\sqrt{\lambda_1}\tilde{E}(1)_2^{(h)}\right] \tag{4.37f}$$

4.6 Discrete equation

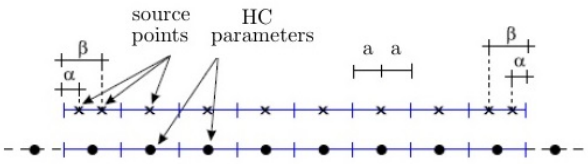

Fig. 4.4. Arrangment of the source points and of HC parameters

Arranging on the discretized contour a number of sources point equal to the number of parameters used in approximate representation 4.4, the expression 4.5 leads to following system of equations

$$\sum_e H_e u_e = \sum_e G_e t_e + b \tag{4.38}$$

where, the contribution of each elements Γ_e to coefficients of the matrices H and G are defined by following the relations

$$H_e = \int_{\Gamma_e} t^{*^T}(\xi, x)\, \phi_e u_e \, d\Gamma e$$
$$G_e = \int_{\Gamma_e} u^{*^T}(\xi, x)\, \phi_e t_e \, d\Gamma e \tag{4.39}$$

the system (4.38) can be re-write as following

$$Hu = Gt + b \tag{4.40}$$

in u and t were collected thr parameters of displacement and traction on the boundary. Basing on the boundary conditions the system can be written in the form

$$Ax = f \tag{4.41}$$

where the matrix A and the vector of known terms f are obtained by rearranging H, G and b, the vector x contains the the unknown quantities of boundary. The system as written can be solved in the unknowns mixed quantities of boundary. It is to be noted that the coefficients matrix compared to the numerical methods of domain discretization is very small and is all full and non-symmetrical. In the previous section has been treated in detail the calculation of integral coefficients that requires special attention, given the presence of singularities in the fundamental solutions.

5

Implementation details

This chapter examines in detail the algorithm implemented in the MATLAB environment. After an introduction to the global quantities, there are reviewed procedures for reading of data, pre-analysis, assembly of the coefficient matrix and boundary solution, domain solution, output by plotting the results. This code provides, for a given geometry of a laminated composite shell, the distribution on the boundary of the tractions and of the displacements. It is also possible to calculate the stresses and the displacements in an individual points of the domain, or in a grid of points, so as to represent globally the results by maps, or level curves.

5.1 Code structure

The structure of the program consists of a series of procedure calls and it is shown in Figure 5.1. After a process of reading data from input via file, first of all it is calculated the compliance and stiffness matrix of the composite and the roots of the characteristic equation and all the quantities involved (SistemSolution). Subsequently, a procedure for pre-analysis imposes boundary conditions and transfers the problem on the working plane. Then, it is assembled the integral coefficient matrix, and the algebraic system is solved within the procedure boundary solution. After getting the boundary solution it is calculated the domain solution on a individual point or on a grid points. The final step consists in management and visualization of the results obtained.

```
% GLOBAL
global LAY lato elemento ele_s ele_e Coord

disp([num2str(toc),'    READ INPUT....'])
test1;

%-------------------------------------------------------------------------%

BuildLaminate;
[C] = AMatrixLaminate(LAY,H);
[lam1,lam2,Delta,A1,A2,D,S] = SistemSolution(C);

%-------------------------------------------------------------------------%

[lato,elemento,ele_s,ele_e]=structures(ele_tot);
disp([num2str(toc),'    PRE-ANALISYS....'])
[elemento,lato] = pre_Analisys(elemento,lato,vinc,npar);
disp([num2str(toc),'    BUILD ELEMENT SOURCE....'])
[ele_s] = elementS(elemento,lato,ele_s);
disp([num2str(toc),'    BUILD ELEMENT FIELD....'])
[ele_e] = elementF(elemento,lato,ele_e);
disp([num2str(toc),'    POST-ANALISYS....'])
[lato] = post_Analisys(lato,vincvalN,vincvalT);
disp([num2str(toc),'    SOLUTION-BOUNDARY....'])
[U,Un,Ut,p,A,UX,UY] = solution_Boundary(lato,ele_e,ele_s,npar,vinc,S,lam1,lam2,A1,A2,D,↙
C);
disp([num2str(toc),'    PARAMETRI....'])
[lato] = parametri(lato);

% --- Procedure for DOMAIN solution starting from BOUNDARY solution  ---%
% --- Generetion of a grid of point ..................... ---%

[grid] = mesh_Grid(densita,distanza);

% grid(1).x=0.001;       %individual point
% grid(1).y=0.999;

n_punti=size(grid,2);
disp([num2str(toc),'    SOLUTION-DOMAIN....'])
[Displ,Stress,Tens] = solution_Domain(ele_e,lato,Un,Ut,npar,H,S,lam1,lam2,A1,A2,D,C,↙
grid,n_punti);

% Plot numerical deformed configuration
disp([num2str(toc),'    PLOT RESULTS....'])
[UX,UY] = plot_def(fac,UX,UY,vinc,vincvalN,vincvalT);
% Stress and Displacement Maps
plot_defo(UX,UY,Displ,grid,n_punti,npar)
plot_sig(Tens,grid,n_punti)
```

Fig. 5.1. Code structure

5.2 Procedures Organization

After introducing the variables involved and after bringing back the calls contained in MAIN, all the phases in which is articulated the algorithm are examined.

5.2.1 Input

At this early stage an m file is built and it will be invoked at the time of reading data. This phase is managed by the procedure ReadInput, which has the task

to read the data contained in a file and store them by variables declared. First of all you provide the four independent elastic characteristics: the Young's modulus in the two direction (1=axis aligned with the fiber direction, 2=axis perpendicular with the fiber direction), the shear modulus and the Poisson's ratio. Then it is provided the number of layers and their orientation respect to the global sistem.

Subsequently it is provided the total number of sides that make up the contour of the shell, the number of internal points where you want to calculate the solution and values the two boundary conditions (assigned traction or displacement). The data provided in subsequent lines identify the coordinates of the vertices of the macroelements. For each vertex is assigned an order number, which serves later, when for every macroelement must indicate the start and end node, as well as the number of elements in which you want to break it. The normal boundary is always considered leaving the domain. For each node are stored both coordinates, while for each macroelement are stored the order numbers of the initial node and the final one, as well as the number of elements in which the user wants to divide. The procedure also stores the coordinates of the internal points where you want to calculate the solution.

5.2.2 Build Laminate - Sistem Solution

In these two procedure, taking in account of elastic characteristics and layers that compose the laminate, it is calculated the complience and stiffness matrix and than you calculate the roots of the characteristic equation and all the quantities involved the fundamental solution.

5.2.3 Pre-Analisys

This phase is mainly engaged to transfer the problem in the plan of calculating. You calculate the length of the macroelements and of their microelements, the normals to the macro and micro elements and the coordinates of every nodes.

5.2.4 Sorce Element

The procedure elemetS receives as input the i-th of the macroelement and the i-th element. This calculates the cosines direction of the outward normal, the number of sources present and their coordinates. All data is stored in the variable ele_s. For each macroelement there are a number of source points equal to the number of HC parameters involved. This number is equal to the number of microelements plus 2 ($n_e + 2$). Their location changes depending on the element type. For the elements that are placed at the extremity there are two source point, one placed at α distance and the other placed β distance (see Figure 4.4). For the other elements the source point is unique and it is placed in the center of the microelement.

5.2.5 Field Element

Also this procedure elemetF takes as input the i-th of the macroelement and the i-th element. It calculates the direction cosines of the outward normal, the number of field point present and their coordinates. All data is stored in the variable ele_e. For each macroelement there are a number of field points equal to the number of microelemts. The field points are placed in the midpoind of every microelemets.

5.2.6 Post-Analisys

This phase is mainly engaged to transfer the boundary conditions.

5.2.7 Boundary Solution

This phase is the core of the code. It is in this phase that it is assembled the system of equations that define the solution of the elastic problem on the contour. The construction of the coefficient matrix is developed through the contributions of all the macroelements and for each of them the contributions of the microelements that constitute it. It is observed that the generation of the equations of the system is developed taking into account that the components of the variables on the contour most convenient to assign the data are normal and tangential and that the evaluation of the integrals is, as already seen, facilitated by the use of a system local reference. This procedure evaluates the effects that the various source points produce in the different field points. The procedure is so divided: a source point that points, counterclockwise, to the field points, you evaluate, referring to the local system of the i-th field point, the distances $\bar{x}$ and $\bar{y}$, the direction cosines (see Figure 4.3). Then, there is another procedure within Boundary Solution: IntegraliCoeff. It calculates the integral coefficients, in analitical way as treated in Section 4.5, to assemble in the system. Each source point fills two rows of the matrix, one for the normal direction and one for the tangential direction. The matrix, that comes out, it is not symmetric a square matrix.

5.2.8 Domain Solution

This phase has the task of deducing the solution in the interior points of the domain as a function of the solution, now known, on the contour. At this stage, in developing the solution on the domain, it is used another procedure that calculate the integral coefficients in the domain: IntegraliCoeff-Domain. This procedure is organized in the same way of the procedure used on the contour.

5.2.9 Plot

These final procedures are needed for a graphics processing of the results. Through them are plotted graph of the displacements, of the stresses and deformed mesh.

6

Numerical Results

A number of cases are presented here to demonstrate the application of the proposed methodology to elastic analysis of 2-D orthotropic medium by the analytical integration of the kernels. The principal material direction are aligned with the Cartesian coordinate directions.

6.1 Test 1: Square plate under uniform load parallel to the fibers

In the first example, an orthotropic square plate is considered, which is subjected to a uniformly distributed load along the principal material direction (see Figure 6.1), and the material properties are listed in Table (6.7). The plate has lenght $100mm$, thickness $1.2mm$ and distribuited load $q = 1MPa$.

The results obtained with the present BEM are compared with the results obtained by Abaqus. In the tables below the comparison of the results between the BEM and Abaqus is presented.

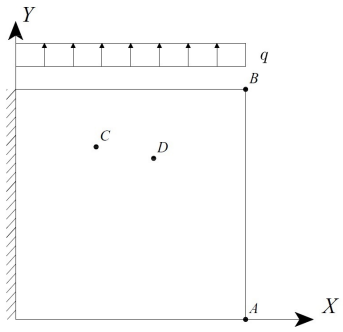

Fig. 6.1. Square plate under uniform load

In the tables (6.1) and (6.2) the comparison of the displacements in the point A, B, C and D is presented. Both the tables refer to the same dof showed in the table (6.1).

Table 6.1. Comparison of the displacements in point A and B between BEM and Abaqus

BEM					**Abaqus**				
N_{el}	L/N_{el}	dof	U_x^A	U_y^B	N_{el}	L/N_{el}	dof	U_x^A	U_y^B
12	$3.33e^{-1}$	40	1.2616	8.2920	9	$3.33e^{-1}$	120	1.1671	6.9620
20	$2.00e^{-1}$	56	1.2226	8.1992	25	$2.00e^{-1}$	288	1.1447	7.4820
132	$3.03e^{-2}$	280	1.1554	8.1722	144	$8.33e^{-2}$	1446	1.1539	7.9279
220	$1.81e^{-2}$	456	1.1555	8.1743	225	$6.66e^{-2}$	2208	1.1557	7.9892
308	$1.29e^{-2}$	632	1.1558	8.1752	400	$5.00e^{-2}$	3843	1.1573	8.0497
396	$1.01e^{-2}$	808	1.1560	8.1756	1089	$3.03e^{-2}$	10200	1.1587	8.1094
484	$8.26e^{-3}$	984	1.1561	8.1759	1600	$2.50e^{-2}$	14888	1.1592	8.1390
604	$6.62e^{-3}$	1224	1.1562	8.1761	4356	$1.51e^{-2}$	39999	1.1598	8.1737
684	$5.84e^{-3}$	1384	1.1563	8.1762	6400	$1.25e^{-2}$	58563	1.1599	8.1830
764	$5.23e^{-3}$	1544	1.1563	8.1763	10000	$1.00e^{-2}$	91203	1.1600	8.1917
844	$4.73e^{-3}$	1704	1.1564	8.1772	12321	$1.00e^{-2}$	112224	1.1600	8.1952
884	$4.52e^{-3}$	1784	1.1565	8.1778	15625	$1.00e^{-2}$	142128	1.1601	8.1987

Table 6.2. Comparison of the displacements in point C between BEM and Abaqus

BEM				**Abaqus**			
U_x^C	U_y^C	U_x^D	U_y^D	U_x^C	U_y^C	U_x^D	U_y^D
−0.2306	3.9991	−0.2707	6.1332	−0.1108	2.4435	−0.1820	4.9246
−0.2202	3.9599	−0.2582	6.0814	−0.1950	3.3046	−0.2401	5.3541
−0.2126	3.9427	−0.2511	6.0614	−0.2093	3.6716	−0.2475	5.8051
−0.2125	3.9431	−0.2510	6.0624	−0.2102	3.7300	−0.2487	5.8649
−0.2125	3.9433	−0.2510	6.0628	−0.2116	3.7886	−0.2497	5.9242
−0.2124	3.9434	−0.2510	6.0631	−0.2128	3.8571	−0.2509	5.9936
−0.2124	3.9435	−0.2510	6.0632	−0.2131	3.8754	−0.2512	6.0121
−0.2124	3.9436	−0.2510	6.0634	−0.2136	3.9093	−0.2516	6.0464
−0.2124	3.9436	−0.2510	6.0634	−0.2137	3.9184	−0.2518	6.0555
−0.2124	3.9437	−0.2510	6.0635	−0.2139	3.9269	−0.2519	6.0642
−0.2124	3.9437	−0.2510	6.0635	−0.2139	3.9303	−0.2519	6.0676
−0.2124	3.9437	−0.2510	6.0635	−0.2139	3.9337	−0.2520	6.0711

In the tables (6.3) and (6.4) the comparison of the stresses in the point C and D is presented. Both the tables refer to the same dof showed in the table (6.1).

Table 6.3. Comparison of the stresses (e^{+1}) in point C,between BEM and Abaqus

BEM			**Abaqus**		
σ^C_{xx}	σ^C_{yy}	τ^C_{xy}	σ^C_{xx}	σ^C_{yy}	τ^C_{xy}
6.2800	−4.4692	−6.1567	4.8108	−4.4279	−8.0257
6.2004	−4.2557	−6.1106	7.0497	−5.2678	−6.5291
6.1959	−4.1623	−6.1400	6.2001	−4.1111	−6.1809
6.1957	−4.1604	−6.1423	6.1914	−4.1919	−6.1827
6.1957	−4.1599	−6.1432	6.1907	−4.1577	−6.1941
6.1957	−4.1597	−6.1437	6.1893	−4.1856	−6.1824
6.1957	−4.1595	−6.1439	6.1904	−4.1802	−6.1856
6.1957	−4.1595	−6.1442	6.1913	−4.1889	−6.1824
6.1957	−4.1594	−6.1443	6.1913	−4.1866	−6.1835
6.1957	−4.1594	−6.1443	6.1915	−4.1875	−6.1833

Table 6.4. Comparison of the stresses (e^{+1}) in point D, between BEM and Abaqus

BEM			**Abaqus**		
σ^D_{xx}	σ^D_{yy}	τ^D_{xy}	σ^D_{xx}	σ^D_{yy}	τ^D_{xy}
5.9857	−2.0406	−4.0729	6.6521	−3.5807	−4.1363
6.0072	−1.9610	−4.0580	5.9620	−1.8496	−4.2436
6.0054	−1.9088	−4.0885	6.0116	−1.9266	−4.1185
6.0057	−1.9077	−4.0912	6.0134	−1.9255	−4.1221
6.0057	−1.9077	−4.0912	6.0111	−1.9123	−4.1360
6.0058	−1.9076	−4.0916	6.0108	−1.9194	−4.1302
6.0058	−1.9075	−4.0918	6.0110	−1.9194	−4.1310
6.0059	−1.9075	−4.0920	6.0109	−1.9218	−4.1293
6.0059	−1.9075	−4.0921	6.0110	−1.9216	−4.1298
6.0059	−1.9075	−4.0922	6.0110	−1.9219	−4.1297

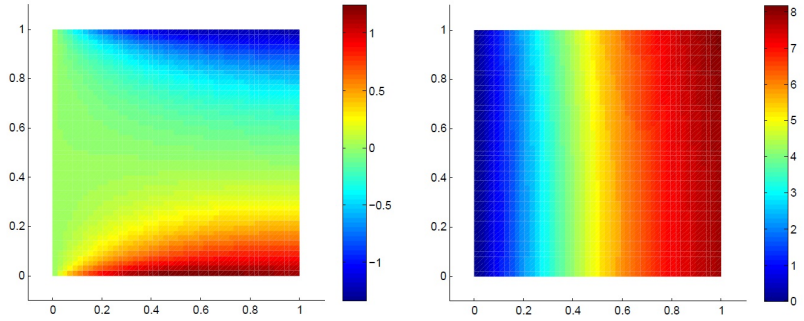

(a) U_x (b) U_y

Fig. 6.2. Displacements in direction X fig.(a) and in direction Y fig.(b)

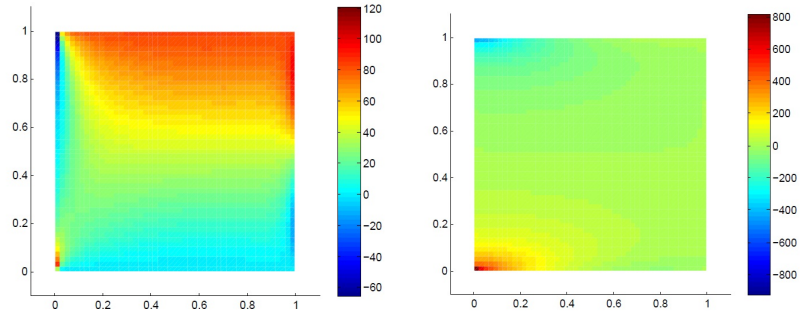

(a) σ_{xx} (b) σ_{yy}

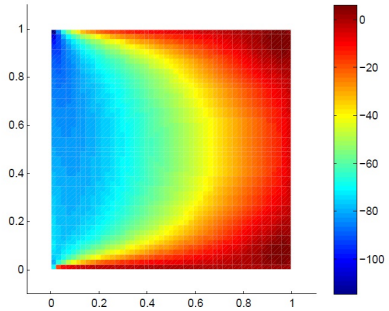

(c) τ_{xy}

Fig. 6.3. Stresses: σ_{xx} fig.(a), σ_{yy} fig.(b) and τ_{xy} fig.(c)

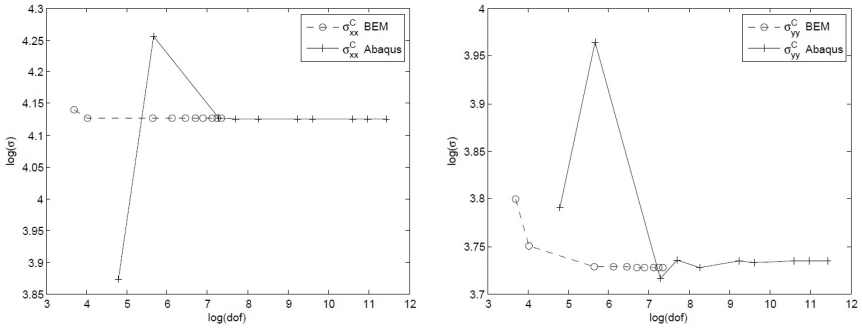

(a) σ^C_{xx}

(b) σ^C_{yy}

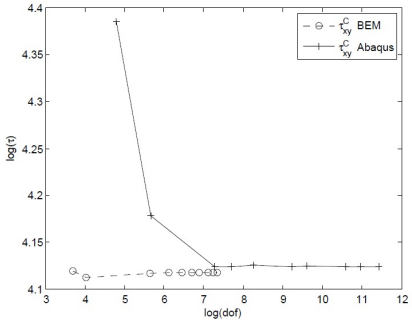

(c) τ^C_{xy}

Fig. 6.4. Convergence of the stresses at point C for increasing dof, σ^C_{xx} fig.(a), σ^C_{yy} fig.(b) and τ^C_{xy} fig.(c)

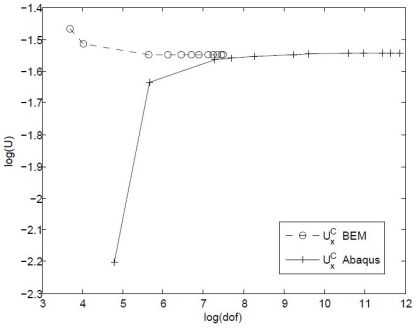

(a) U^C_x

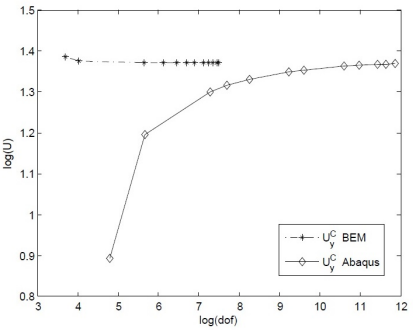

(b) U^C_y

Fig. 6.5. Convergence of the displacements at point C for increasing dof

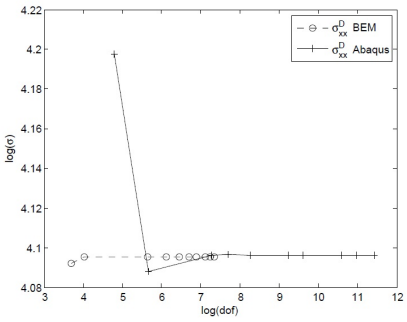

(a) σ_{xx}^D

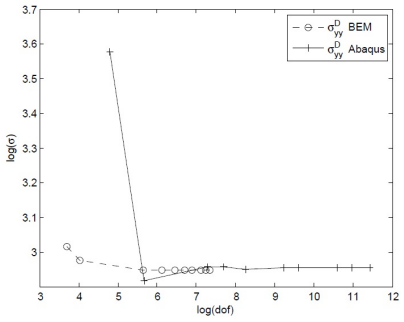

(b) σ_{yy}^D

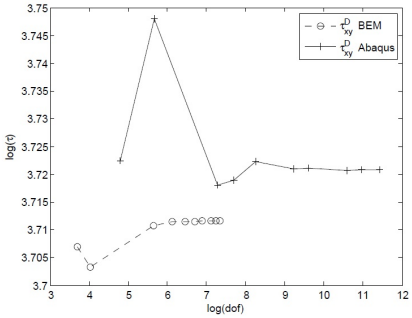

(c) τ_{xy}^D

Fig. 6.6. Convergence of the stresses at point D for increasing dof, σ_{xx}^C fig.(a), σ_{yy}^C fig.(b) and τ_{xy}^C fig.(c)

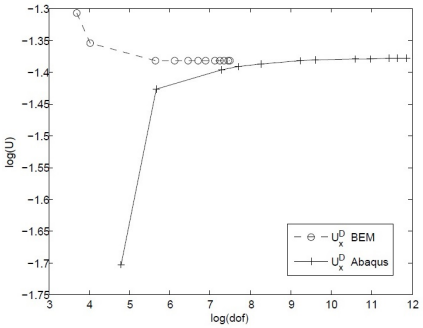

(a) U_x^D

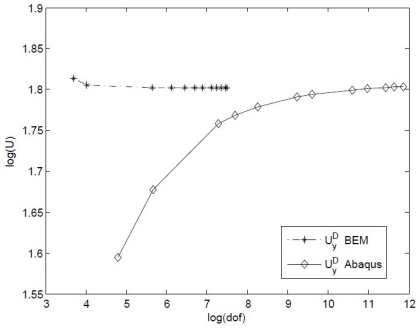

(b) U_y^D

Fig. 6.7. Convergence of the displacements at point D for increasing dof

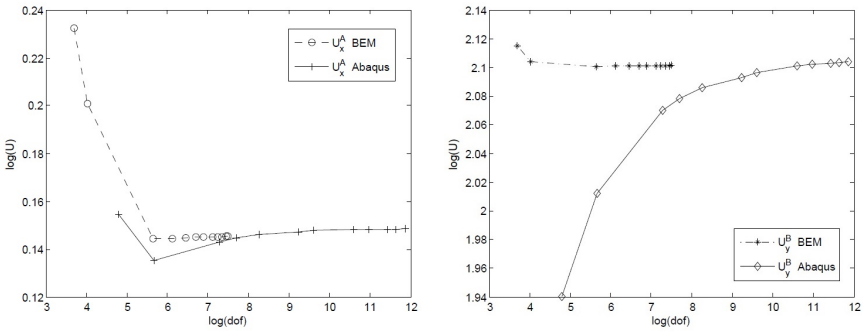

(a) U_x^A (b) U_y^B

Fig. 6.8. Convergence of the displacements at point A and B for increasing dof, U_x^A fig.(a) and U_y^B fig.(b)

6.1.1 Test 2: Cantiliver plate under uniform shear load perpendicular to the fibers

In the second example, an orthotropic cantilever is considered, which is subjected to a uniformly shear distributed load perpendicular to the fiber direction (Figure 6.9), and the material properties are listed in Table (6.8). The plate has lenght $L = 200mm$, height $h = 10mm$, thickness $t = 1mm$ and distribuited shear load $q = 0.03MPa$.

In this case, to ensure a correct modeling, in dividing the edge in the boundary element, yo have to take in account of the relationship between the geometric dimensions. So, the number of elements on the base will be 20 times higher than that of the height.

The results obtained with the present BEM are compared with the results obtained by Abaqus. In the in Table (6.5) it is possible to compare the results of the BEM code and of Abaqus for the points A and B.

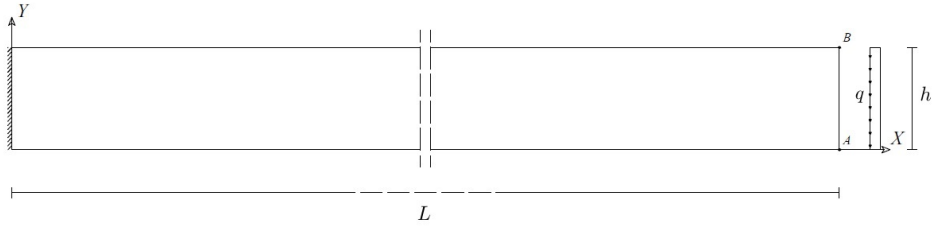

Fig. 6.9. Cantilever plate under shear uniform load

Table 6.5. Comparison of the displacements in point A and B between BEM and Abaqus

BEM					**Abaqus**				
N_{el}	L/N_{el}	dof	U_y^A	U_x^B	N_{el}	L/N_{el}	dof	U_x^A	U_y^B
126	$3.33e^{-1}$	268	−111.2928	4.1529	180	$3.33e^{-1}$	2001	−113.3769	4.2317
210	$2.00e^{-1}$	436	−112.0300	4.1797	500	$2.00e^{-1}$	5133	−113.4735	4.2343
378	$1.11e^{-1}$	772	−112.6496	4.2017	1080	$1.66e^{-1}$	9222	−113.5099	4.2353
462	$9.09e^{-2}$	940	−112.7832	4.2065	2000	$1.00e^{-1}$	19263	−113.5457	4.2363
630	$6.66e^{-2}$	1276	−112.9307	4.2117	2420	$9.00e^{-2}$	23379	−113.5524	4.2364
798	$5.26e^{-2}$	1612	−113.0072	4.2144					
1050	$4.00e^{-2}$	2116	−113.0689	4.2166					
1302	$3.22e^{-2}$	2620	−113.1027	4.2178					
1638	$2.56e^{-2}$	3292	−113.1288	4.2188					
1890	$2.22e^{-2}$	3796	−113.1411	4.2192					
2310	$1.81e^{-1}$	4636	−113.1546	4.2197					
3234	$1.29e^{-1}$	6484	−113.1700	4.2202					

In the table (6.6) the comparison of the stresses in the point C is presented. The table refer to the same dof showed in the table (6.2).

Table 6.6. Comparison of the stresses (e^{+1}) in point C,between BEM and Abaqus

BEM			**Abaqus**		
σ_{xx}^C	σ_{yy}^C	τ_{xy}^C	σ_{xx}^C	σ_{yy}^C	τ_{xy}^C
27.8540	−60.6732	−1.0229	4.8108	1.0380	0.0079
26.9547	−43.6052	−0.8924	3.8224	1.0869	0.0062
23.6634	−26.7278	−0.7609	3.8820	1.1055	0.0059
22.1997	−22.3126	−0.7276	4.0875	1.1646	0.0057
19.8868	−16.7807	−0.6887	4.1347	1.1775	0.0058
18.1981	−13.4720	−0.6685			
16.4052	−10.4281	−0.6539			
15.1562	−8.5273	−0.6483			
13.9865	−6.8753	−0.6470			
13.3432	−6.0086	−6.4851874			

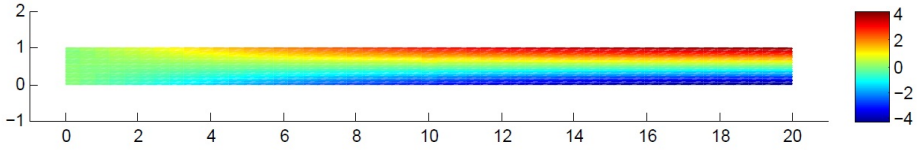

(a) U_x

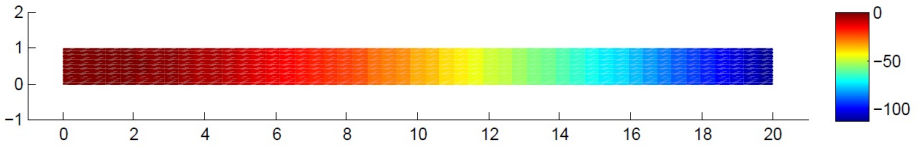

(b) U_y

Fig. 6.10. Displacements in direction X fig.(a) and in direction Y fig.(b)

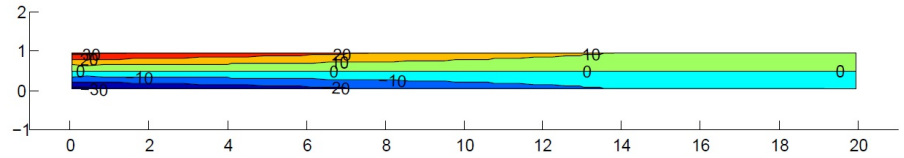

(a) σ_{xx}

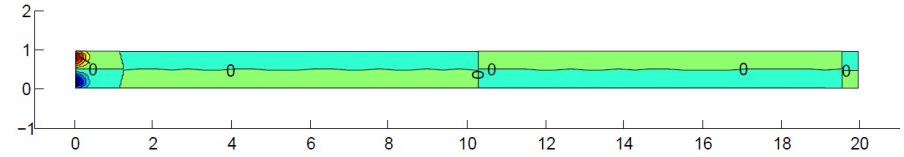

(b) σ_{yy}

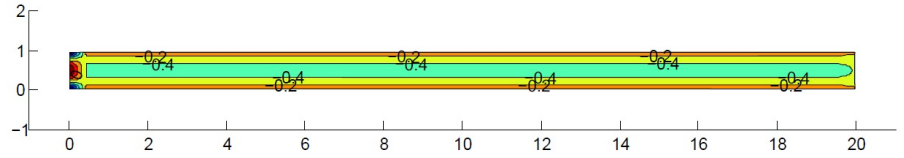

(c) τ_{xy}

Fig. 6.11. Stresses: σ_{xx} fig.(a), σ_{yy} fig.(b) and τ_{xy} fig.(c)

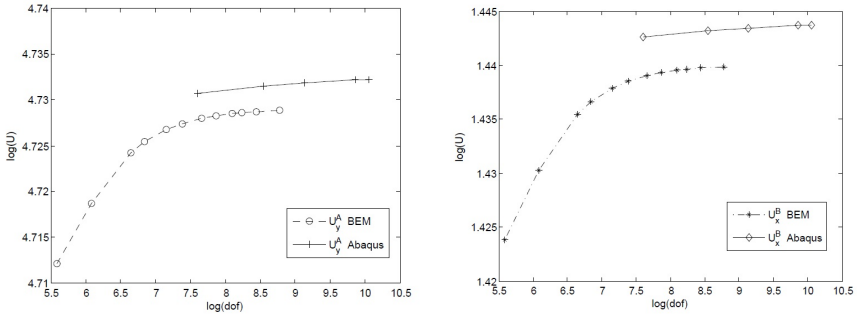

(a) U_y^A (b) U_x^B

Fig. 6.12. Convergence of the displacement for increasing dof, in point A U_y^A fig(a) and in point B U_x^X fig(b)

6.1.2 Material properties

Table 6.7. Material properties

Elastic constants (MPa)		Layer n°	Orientation
E_1	161.00	1	90
E_2	90.27		
ν_{12}	0.28		
G_{12}	7.17		

Table 6.8. Material properties

Elastic constants (MPa)		Layer n°	Orientation
E_1	85.0	1	0
E_2	84.0		
ν_{12}	0.3		
G_{12}	10.0		

Conclusions

At the conclusion of this thesis highlights some significant aspects of the experience took place. As regards the formulation of the plane stress problem in the case of orthotropic constitutive equation, it should be noted that, the problem is solved taking into account the orthotropic constitutive equation precisely and then generating of the fundamental solutions specific for this case. Based on this, the fundamental solutions for the isotropic case may be obtained by downgrading the orthotropic constitutive equation and making a passage to the limit.

In reference to the interpolation used were obtained expressions of functions HC. As for the analytical evaluation of the integral coefficients goes highlighted the efficiency of the implementation. All contributions are expressed as a function of a few recurring integrals, defined recursively. The results presented in the Chapter 6 show the performance obtained with the model boundary elements developed. The representation of the stress, has proved an effective tool for immediate visualization of the stress state, as well as the representation for contour lines. The code shows the limit of the FEM models. When there are stress concentration the BEM is much more reliable compared with the FEM. The accuracy of the results was validated by comparison with the program Abaqus. The accuracy of the code is determined primarily by the analytic integration of the coefficients and by the interpolation of mechanical quantities, which is effective even with a few elements.

Another interesting fact is that thanks to the integration of analytical integral contributions you can evaluate the solution at points very close to the boundary, without triggering instability in the code. The solution within the domain can be evaluated pushing closer to the boundary up to an order of magnitude of e^{-9} respect to the length of the element.

References

[1] R. J. Rizzo and D. J. Shippy. "A method for stress determination in plane anisotropic elastic bodies". In: *Composite materials* 4 (1970), pp. 36–61.

[2] G. Szeidl and J. Dudra. "BEM formulation for plane orthotropic bodies - a modification for exterior regions and its proof". In: *Periodica Polytechnica* 51.2 (2007), pp. 23–35.

[3] L. Huang, X. Sun, Y. Liu, and Z. Cen. "Parameter identification for two-dimensional orthotropic material bodies by the boundary element method". In: *Engineering Analysis with Boundary Elements* 28.2 (2004), pp. 109–121.

[4] M. Aristodemo and E. Turco. "A boundary element procedure for the analysis of two-dimensional elastic structures". In: *Boundary Integral Methods: theory and applications* 37 (1990), pp. 65–74.

[5] M. Aristodemo and E. Turco. "Boundary element discretization of plane elasticity and plate bending problems". In: *International journal for numerical methods in engineering* 37 (1994), pp. 965–987.

[6] J. N. Reddy. *Mechanics of laminated Composite Plates and Shells, Theory and Analysis*. Second. Department of Mechanical Engineering at Texas A&M University, College Station, Texas, US. CRC Press, 2004.

[7] E. J. Barbero. "Handbook of Composites". In: ed. by Stan Peters. 2nd. Thompson Science/Chapman & Hall, 1998. Chap. Chapter 46: Construction, pp. 982–1003.

[8] E. J. Barbero. *Finite Element Analysis of Composite Materials*. First. `http://barbero.cadec-online.com/feacm`. Taylor & Francis, 2008.

[9] E. J. Barbero. *Introduction to Composite Materials Design*. Second. `http://barbero.cadec-online.com/icmd`. Philadelphia, PA: CRC Press, 2011.

[10] J. T. Katsikadelis. *Boundary Elements Theory and Applications*. First. Department of Civil Engineering, National Technical University of Athens, Athens, Greece. Elsevier, 2002.

[11] C.A. Brebbia and J. Dominguez. *Boundary Elements: an introductory course*. First. London. McGraw-Hill Incorporated, 1989.

[12] C.A. Brebbia, J.C.F Telles, and L.C Wrobel. *Boundary element techniques*. First. Berlin. Springer-Verlag, 1984.

[13] F. Hartmann. *Introduction to Boundary Elements: Theory and Applications*. First. University of Dortmund Department of Civil Engineering, Dortmund, german. Springer-Verlag, 1989.

[14] P.K. Banerjee and R. Butterfield. *Boundary element methods in engineering science*. First. McGraw-Hill, 1981.

[15] R. J. Rizzo. "An Integral Equation Approach to Boundary Value Problems of Classical Elastostatics". In: *Quarterly of Applied Mathematics* 25 (1967), pp. 83–95.

[16] M. Aristodemo. “A High-Continuity Finite Element Model for Two Dimensional Elastic Problems”. In: *Computers & Structures* 21 (1985), pp. 987–993.